Controlling molecular chirality and motion

van Delden, Richard Andreas

Chapter 2

Donor-Acceptor Substituted Chiroptical Molecular Switches

This chapter deals with the synthesis and properties of chiroptical molecular switches based on donor-acceptor substituted sterically overcrowded alkenes. Physical properties of these photochromic compounds are discussed and a number of new derivatives are presented. These include the most efficient overcrowded alkene based molecular switch developed thus far, for which it is possible to control molecular chirality in a highly stereoselective manner. In addition, some simplified analogues are reported that were used to study the separate influences of the donor and the acceptor substituent. A novel synthetic approach to allow rapid construction of a variety of these donor-acceptor type systems is introduced. This synthetic methodology is based on a palladium-catalyzed aromatic substitution reaction on a bromo-substituted sterically overcrowded alkene.

2.1 Introduction

Chiroptical molecular switches based on two pseudoenantiomeric forms of an intrinsically chiral helix-shaped sterically overcrowded alkene form a unique class of the different types of chiral photochromic switches known today. They were introduced in the previous chapter. It is one of the few types of chiral switches where the chirality itself is switched upon photoexcitation. Most other examples are based on structures in which the chiral part and the switching unit are two separate entities. Here, switching itself does not influence the chirality of the system but merely results in a geometrical change leading to a change in chiral properties, *i.e.* optical rotation, circular dichroism, or chiral perturbation by a given compound on its surroundings. In most examples of chiral photochromic compounds, the properties of the two distinct states of a molecular switch are completely different. For most compounds in the switching event even chemical bonds are rearranged, leading to completely different isomers. When light is used as a stimulus for both the forward and the reverse process, the totally different absorption spectra of the two isomers ensures high selectivity. Very illustrative in this case is the change in molecular structure upon photochemical isomerization of a diarylethylene switch, starting from a hexatriene system in the open form to a cyclic hexadiene system in the closed form. In an extreme case, the dithienyl switching unit is asymmetrically functionalized with an electron donating 2-benzo[1,3]dithiol-2-ylidenemethyl-group on the 2-position and an electron withdrawing dicyanovinyl-group on the 2'-position as illustrated for **2.1** (Scheme 2.1).[1] With this *push-pull* system it is possible to use remote wavelengths of light for switching (although due to the absence of a chiral influence no stereocontrol is possible).

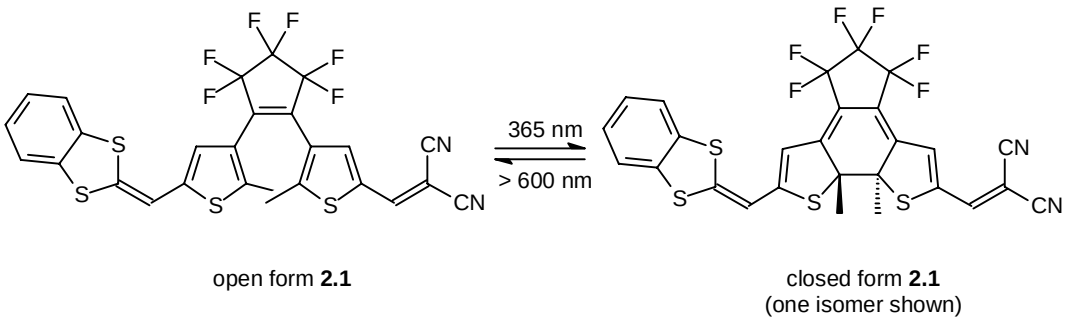

Scheme 2.1 A donor-acceptor substituted diarylethylene switch.

In the closed form, the two chromophores of opposite electron affinity are in full conjugation whereas in the open form the conjugation between the two chromophores is absent. As a result, the open form shows UV-VIS absorptions up to about 500 nm. Due to overlapping absorptions of open and closed form apparent from the UV-VIS spectra, only wavelengths up to approximately 400 nm can be used for efficient forward switching. Upon photochemical ring closure a new UV-VIS band appears with a maximum around 800 nm as a result of increased conjugation length. This broad UV-VIS band with at least 200 nm half-width and ranging up to approximately 1000 nm corresponding to near-infrared is clearly indicative of a charge transfer band. As a result, wavelengths up to at least 900 nm can be used to induce

ring opening in the reverse photoisomerization process. It is superfluous to note that irradiation with light of wavelengths this far outside the absorption range of the open form results in an efficient reverse process.

As already mentioned in Chapter 1 our chiroptical molecular switches based on sterically overcrowded alkenes use a stilbene-type *cis-trans* isomerization as the switching process. Closer investigation of the two stable forms of the molecule, which are named *cis* and *trans* by virtue of the relative position of the upper half compared to an asymmetrically (mono- or di-) functionalized lower half, show that both forms combine the properties of *cis*- and *trans*-stilbene. Forward and backwards switching involves a similar process and thus similar absorption characteristics can be expected for the two states of the switch. Indeed, sterically overcrowded alkenes bearing only electronically neutral substituents show inefficient if any switching behavior. Even the first reported chiroptical molecular switch, where the lower half of the molecule was asymmetrically substituted with an electron-donating methoxy-substituent due to monosubstitution at the 2-position (compound **1.12**, Scheme 1.10), resulted in a difference in diastereomeric excess of only 8% with the *cis*-isomer in excess in both cases. It seems that for sterically overcrowded alkenes to function as efficient chiroptical molecular switches, asymmetric donor-acceptor substitution is essential. For a different situation with molecular motors based on sterically overcrowded alkenes, see Chapter 5.

2.2 Donor-Acceptor Substituted Molecular Switches

The highly efficient switchable parent compound for all the donor-acceptor systems developed in our laboratories is the dimethylamine nitro-substituted chiroptical molecular switch **2.2** (same as compound **1.13**). With this molecular system (where the two enantiomeric switch combinations ((*M*)-*cis* / (*P*)-*trans* and (*P*)-*cis* / (*M*)-*trans*) have to be resolved by chiral chromatographic techniques) switching between a photostationary state (PSS) of 90% (*M*)-*cis*-**2.2** and 10% (*P*)-*trans*-**2.2** using 435 nm light and 30% (*M*)-*cis*-**2.2** and 70% (*P*)-*trans*-**2.2** using 365 nm light is possible in *n*-hexane solution (Scheme 2.2).[2] Due to the asymmetric donor-acceptor substitution in the lower half not only the switching efficiencies of the system have dramatically increased compared to other sterically overcrowded alkenes, but also charge transfer type bands appear in the UV-VIS spectra of both forms. There is the possibility of charge separation, most probably via the sulfur atom (in the lower half of **2.2**) resulting in a considerable red shift in the absorption spectra. This bathochromic shift allows photoswitching at longer wavelengths, that is lower energies of irradiation, which will increase the fatigue resistance and make the entire process more energetically efficient provided that quantum yields for switching remain the same. It was possible to perform 80 switching cycles without deterioration or racemization. The composition of the photostationary states, and as a consequence the excess of (*M*)- or (*P*)-helices is, however, strongly dependent on the medium (*n*-hexane was proven to be the best solvent for this system).

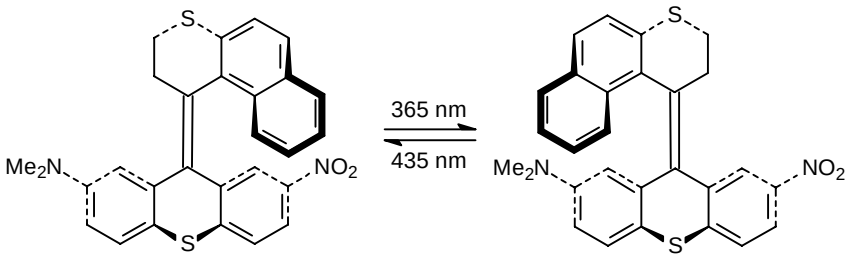

(*M*)-*cis*-**2.2** (*P*)-*trans*-**2.2**

Scheme 2.2 Donor-acceptor substituted chiroptical molecular switch **2.2** showing high stereoselectivity.

With this system molecular chirality can efficiently be controlled by changing only the wavelength of light used. A number of other donor-acceptor substituted systems based on the same molecular skeleton, developed in our group include a compound similar to **2.2**, where only the electron-donating substituent has changed from a dimethylamino- to a methoxy-substituent.[3] Using Hammett substituent constants (either σ_p or σ^+_p) as a measure for donor strength, this means a decrease in the electron donating power by a factor of approximately 2.2.[4] Unfortunately, however, due to poor solubility, poor resolution and an observed hypsochromic shift of the UV-VIS spectra (which is in accordance with the anticipated decreased donor-acceptor interaction) the switching selectivity was never measured. A decreased switching selectivity can be expected, however.

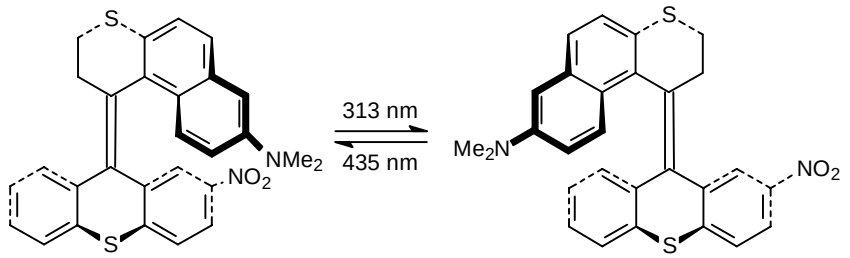

(*M*)-*cis*-**2.3** (*P*)-*trans*-**2.3**

Scheme 2.3 Alternative chiroptical molecular switch **2.3** with donor in upper half and acceptor in lower half of the molecule.

In a third system developed in our group, not the nature of the donor-acceptor substituents was changed but rather the relative position of the two substituents. By introducing a dimethylamino-substituent in the upper half of the molecule as present in compound **2.3** the difference between the two isomers was expected to increase. In case of (*M*)-*cis*-**2.3**, where the donor and acceptor substituents are close together, a strong dipolar interaction between the donor and acceptor moieties is expected. This possibility for this direct interaction is absent in case of (*P*)-*trans*-**2.3** and as a consequence switching would be more efficient. The difference between the two isomers has indeed increased, as observed from UV and CD absorption spectra. Efficient photoisomerization was only observed in one direction strongly depending on solvent polarity. In toluene, for example, a remarkable *cis* : *trans* ratio of 99 : 1 was found for the photostationary state at 435 nm but switching to a state of excess *trans*-**2.3** was only possible in a highly polar solvent as dichloromethane and even then a *trans* : *cis*

ratio of only 55 : 45 was achieved at 313 nm. To explain both the high selectivity in switching for compound **2.2** as well as the high *cis* to *trans* efficiency for compound **2.3** a closer look at the photophysical processes involved in these systems is necessary.

2.2.1 Physical Properties and Switching Efficiency

In a switching process, which is based on the difference in UV-VIS absorption of two states of a molecular switch, the switching efficiency is linearly related to the ratio of the two UV-VIS absorptions by Equation 2.1. The ratio of the two extinction coefficients at a certain wavelength determines the ratio of the two switch states in a photostationary state. To put it in general terms, if at a certain wavelength one (*cis*) of the two forms (*cis* and *trans*) absorbs more of the light, this monochromatic light will preferentially excite this (*cis*) form leading to a photostationary state where the other form (*trans*) is present in excess. A second property determining the efficiency of the switching process is the ratio of the quantum yields (Φ) for interconversion of the two forms. This quantum yield indicates the number of photons that is used for the actual isomerization of the system. When one of the two directions of isomerization (*cis*→*trans*) is more efficient than the other (*cis*←*trans*) this will also lead to a photostationary state where one of the isomers, in this case the *trans*-form, is present in excess. From Equation 2.1 the possibility arises that these two effects will compensate.

$$\frac{[cis]}{[trans]} = \frac{\varepsilon_{trans}}{\varepsilon_{cis}} \times \frac{\Phi_{trans \rightarrow cis}}{\Phi_{cis \rightarrow trans}} \qquad (2.1)$$

For a photochromic switch where different wavelengths of light are employed for switching, the ratio of the two, in our case *cis* and *trans*, stereoisomers should be strongly wavelength dependent. At different wavelengths, the photoequilibrium should prefer either the *cis*- or the *trans*-state. Quantum yields of isomerization, since they reflect the excited (transition) state are expected to be largely wavelength independent, so unless different excited states can be reached by using different excitation wavelength, this quantum yield factor will never be the conclusive factor for reversible switching. As is well known from UV-VIS spectroscopy, the extinction coefficient of any given compound is extremely wavelength dependent. Also the ratio of the two extinction coefficients of a photochromic switch is wavelength dependent and this is the factor determining the switch efficiency. Asymmetric substitution of the molecular skeleton, as in the case of compound **2.2**, results in subtle differences in the UV-VIS spectra of the two pseudoenantiomeric forms. These subtle differences are far smaller than for the diarylethylene example given above but can nevertheless be used for efficient switching.

Clearly visible from Figure 2.1, there are maximums in the ratio of extinction coefficients of the two pseudoenantiomers at 365 and 435 nm. According to equation 2.1 this implies that these wavelengths are the most ideal wavelengths for switching as was experimentally confirmed.

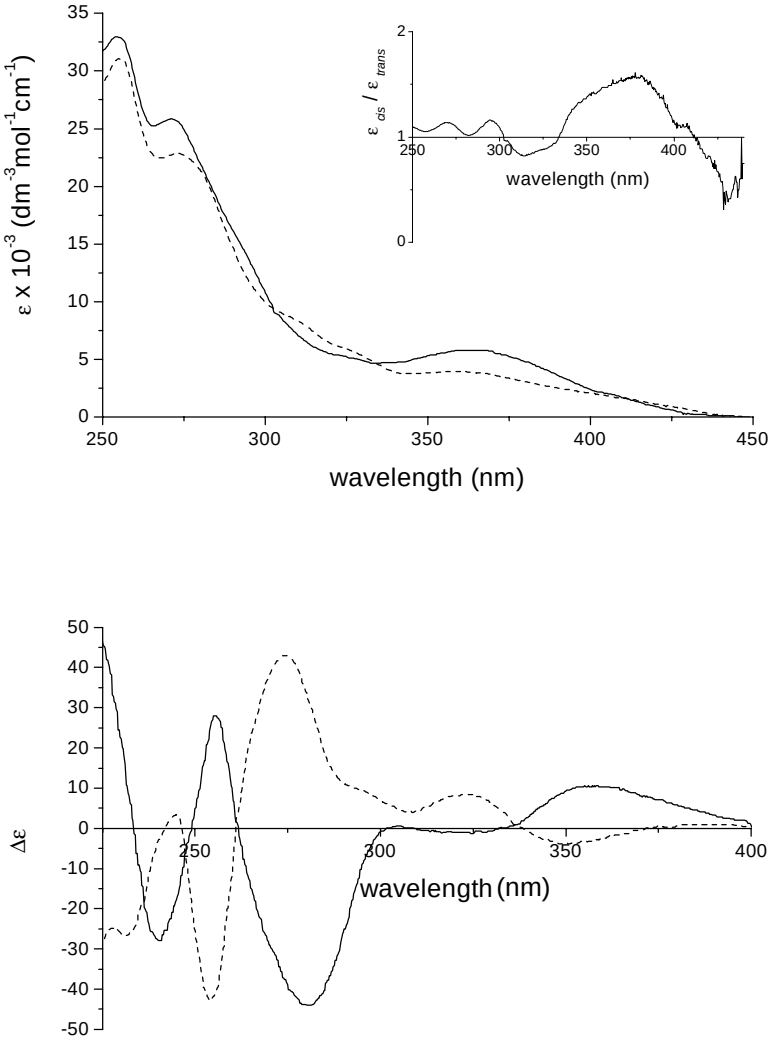

Figure 2.1 UV-VIS (top) and CD (bottom) absorption spectra of donor-acceptor switch **2.2** together with the ratio of the two extinction coefficients (ε_{cis} / ε_{trans}, inset). The solid lines correspond to (*M*)-*cis*-**2.2** and the dashed graphs to (*P*)-*trans*-**2.2.**

Of utmost importance for chiroptical switching is the pseudoenantiomeric relationship between the two isomers since we want to exploit the opposite chiral behavior. This pseudoenantiomeric relation is most conveniently shown by the relative CD spectra of the two forms also depicted in Figure 2.1. The near mirror-image chiral properties, indicative of a pseudoenantiomeric relationship are clearly visible. These two effects of designing a molecular systems with at the same time a maximal difference in UV absorption and minimal deviation from mirror-image CD absorption are competitive and have to be balanced in order to develop an efficient chiroptical molecular switch. An important characteristic of these chiroptical switches is the possibility to execute the writing, reading and erasing cycle with a single physical method. Apart from writing (UV-VIS) and reading (non-destructive by optical rotary dispersion (ORD) remote from the switching wavelengths) these chiral photochromic materials might be employed for an EDRAW (Erasable Direct Read After Write) protocol.[5]

In case of compound **2.3** the UV absorption shows similar subtle differences between the two forms. Nevertheless, from CD spectroscopy it follows that while the *cis*-isomer shows CD bands which in magnitude resemble the ones found for compound **2.2**, the *trans*-isomer shows strongly decreased values for $\Delta\varepsilon$.[3] A second factor preventing it from becoming a suitable candidate for actual switching applications is the preference for the *cis*-isomer throughout the entire wavelength spectrum and in almost any solvent. In this case apparently the quantum yield ratio is the predominant factor in the switching efficiency. Due to favorable donor-acceptor interaction the excited state will predominantly show a *cis*-like geometry leading to a *cis*-enriched ground state only slightly dependent on the wavelength used for excitation. This assumption is supported by the fact that in more polar solvents where intramolecular dipole interactions become less important the photostationary states are increasingly shifted to the *trans*-isomer.

Although these major drawbacks associated with compound **2.3** will prevent it from being a successful chiroptical molecular switch, it can in principle be used in a write-once type of protocol where starting from the *trans*-state information is written very efficiently with up to 99:1 diastereomeric ratio, in toluene solution in preference of the *cis*-state. In the *cis*-state the written information is stable to irradiation over a broad range of wavelengths since almost all investigated photostationary states had the *cis*-isomer as the major isomer. For data storage application this *locking* of information is of great importance but here the systems suffers from the fact that although the *cis*-form is relatively stable to irradiation, the *trans*-form will eventually also be converted to the *cis*-form thereby losing stored information.

2.2.2 Gated Photoswitching and Photoswitching of Luminescence

As stated, locking of written information is absolutely essential for optical data storage; a locking and unlocking mechanism might even result in rewritable systems. This property is called gated response and implies the necessity of using a second external stimulus in order to allow switching in these types of molecules.[6] A number of chemically gated systems, in which the photochromic event and for instance fluorescence, ion binding or electrochemical properties are mutually regulated, have been reported.[7] N. Huck showed that donor-acceptor switch **2.2** by the presence of a basic dimethylamino-substituent also allows gated photoswitching (Scheme 2.4).[8] The photochemical isomerization process of both (*M*)-*cis*-**2.2** and (*P*)-*trans*-**2.2** was effectively blocked by the addition of trifluoroacetic acid. Protonation of the dimethylamine donor unit changes the lower half of the molecule from a *push-pull* donor-acceptor system to a *pull-pull* acceptor-acceptor system (nitro and ammonium cation). As a consequence, photoisomerization is completely blocked rather than that the absence of a donor-acceptor system leads to less efficient isomerization. It seems that in the excited state of these molecules the cationic center acts as an energy drain allowing a fast additional relaxation pathway to compete with and completely block the photoisomerization. The photoisomerization behavior can be restored upon subsequent deprotonation by the addition of base e.g. triethylamine. This protonation-deprotonation protocol does not only lead to gated response but also has an effect on the fluorescence of the molecule, leading to a dual-mode photoswitching of luminescence. This might be used as a, by definition destructive but highly sensitive, read-out tool.

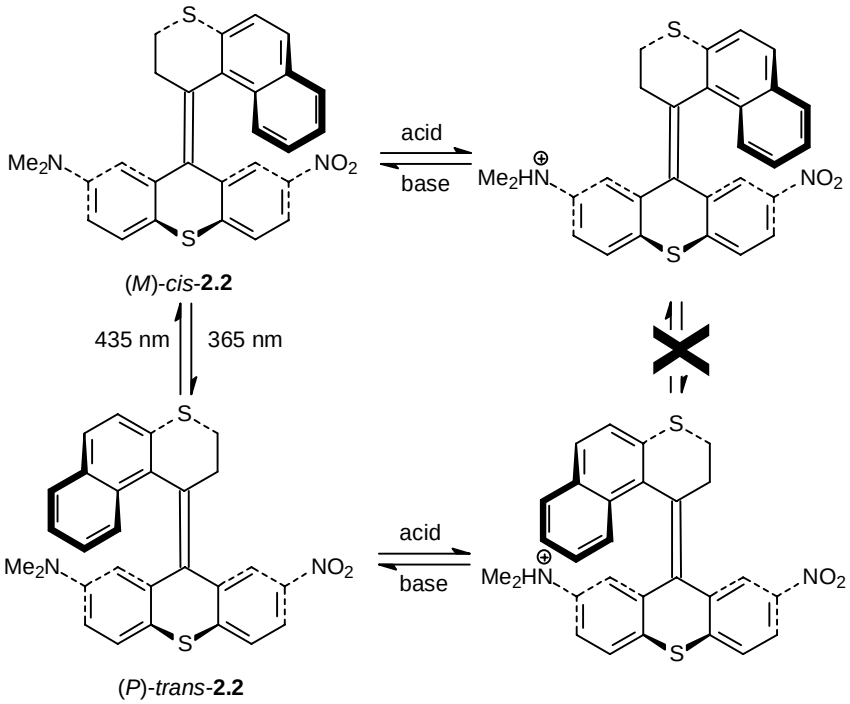

Scheme 2.4 Blocking isomerization by protonation allowing gated photoswitching.

Photomodulation of emission between a relatively weak fluorescent state for (*M*)-*cis*-**2.2** at 528 nm and a relatively strong fluorescent state for (*P*)-*trans*-**2.2** at 531 nm was shown upon switching in *n*-hexane. The fluorescence was found to be highly solvent dependent. Protonation of these photochromic compounds resulted in complete quenching of the emission for both forms whereas after deprotonation fluorescence intensities were fully recovered.[9] Combined, this allows for switching between three fluorescent states *on* (*trans)*, *dimmed* (*cis*) and *off* (both protonated forms) by simultaneous use of light and acid/base stimuli. Remarkably, using time-resolved fluorescence spectroscopy and measuring circularly polarized luminescence, it was found that the chirality of the fluorescent excited states strongly depends on the polarity of the solvent.[10] In *n*-hexane, both (*M*)-*cis*-**2.2** and (*P*)-*trans*-**2.2** show the same sign of circularly polarized luminescence ($g_{lum} = -4.2 \times 10^{-4}$) while in benzene circular polarization of luminescence is opposite for (*M*)-*cis*-**2.2** ($g_{lum} = +5.6 \times 10^{-4}$) and (*P*)-*trans*-**2.2** ($g_{lum} = -7.8 \times 10^{-4}$). This result can be explained by the existence of a mutual *trans*-like luminescent excited state in *n*-hexane, where in benzene clearly a *cis*-like and a *trans*-like excited state can be observed.

A change in fluorescence emission of the different forms involved in the photochromic system has been observed in a number of multifunctional switches. An on/off switching of emission was found in the binaphthol-based indolylfulgide chiral photochromic system.[11] Another interesting example concerns a paracyclophane substituted with two chiral camphanic acid moieties. In this case the photochemical interconversion in one direction is accompanied by circularly polarized chemiluminescence.[12] Lehn *et al.* found strong emission in the open form of a diarylethene-based switch whereas the closed form showed only weak fluorescence.[13] It was expected that the use of the same type of protocol for compound **2.3** should have large consequences. Protonation of the dimethylamino donor substituent again

changes this group into an ammonium cation acceptor substituent leading to unfavorable acceptor-acceptor interactions in the *cis*-state which could result in more efficient switching toward the *trans*-isomer. However, again in this case protonation was shown to completely prevent the isomerization process (Scheme 2.5).[14] Nevertheless, this protonation allows the use of this compound in a write-once switching protocol already implied above. The written information can effectively be stored by protonation of the molecular data storage units.

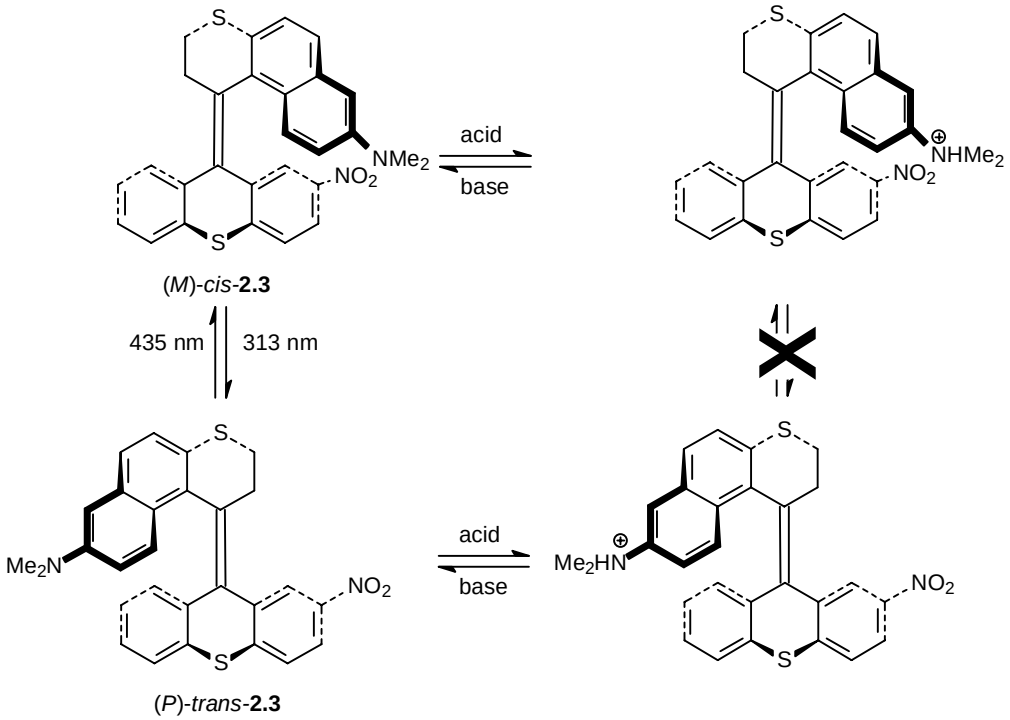

Scheme 2.5 Blocking isomerization upon protonation for compound **2.3**.

2.2.3 Drawbacks and Strategy

Photoresponsive system **2.2** fulfils several of the requirements for an efficient switch, formulated in the previous chapter. The reversibility during a large number of cycles remains to be established. Another critical issue for application in any information storage system is the response time. It was shown by using ultrafast laser spectroscopy that the *cis-trans* isomerization in overcrowded alkenes takes place in microseconds and the isomerization mechanism probably involves a strongly polar twisted phantom state.[15] The actual observed switching times merely reflect the time needed for full equilibration of the system to form the photostationary state rather than the *cis* to *trans* isomerization itself. On the basis of available photochemical data it appears that high speed switching is precluded when the chiroptical switches are incorporated in polymer matrices. For compound **2.2** going from *n*-hexane solution to a PMMA polymer matrix necessary irradiation times increased by a factor of 100 from about 30-60 sec in solution[16] to about 1 h in the polymer film.[17]

The major drawback from a molecular point of view is the relatively low switching efficiency towards the *trans*-side of the photoequilibrium. The strategy based on the asymmetric donor-acceptor substitution pattern proved to be efficient and the dialkylamine and nitro-

substituents proved to be suitable for this purpose. Because of synthetic reasons and because of their relatively large electron-donating and withdrawing strengths, further improvement of this system would require subtle adjustments on the molecular system. A second drawback, which becomes of considerable importance especially when the molecule is used in a liquid crystalline environment, is the low solubility of the compound in organic solvents and low compatibility in liquid crystalline matrices (Chapter 3). This low solubility leads to inefficient resolution and the low compatibility leads to severe limitations with respect to the applicability of the system in organized matrices. In a novel design, merely in order to overcome this second drawback, one of the N-methyl groups is replaced by an *n*-hexyl group and solubility and compatibility are expected to increase considerably for compound **2.4** (Figure 2.2). Although subtle, this slight modification of the donor substituent also proved to have an effect on the switching efficiency.

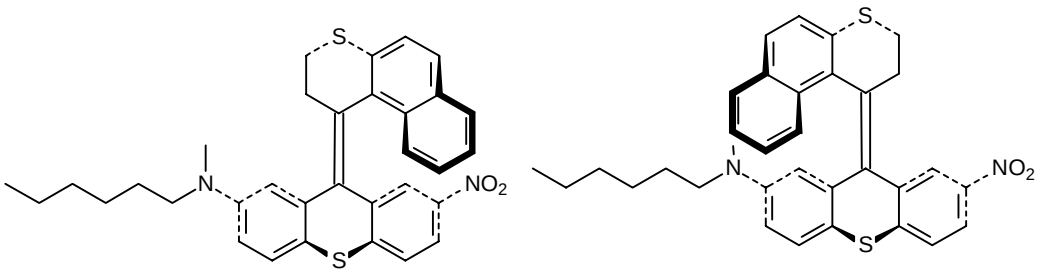

(*M*)-*cis*-**2.4** (*P*)-*trans*-**2.4**

Figure 2.2 *n*-Hexyl functionalized donor-acceptor target molecule **2.4**.

2.3 Synthetic Strategy

B. de Lange in our group developed a suitable and reasonably efficient synthesis of sterically overcrowded alkenes.[18] The crucial step in this synthesis is the formation of the central, sterically demanding, double bond. Where most commonly used olefinic bond forming reactions, like, for example, McMurry coupling reactions, Wittig type alkene formation and Peterson olefination failed to form these overcrowded structures, the diazo-thioketone coupling method[19] was successful. This approach is illustrated for compounds **2.4** in Scheme 2.6. By connecting the upper (hydrazone) **2.5** and lower (thioketone) **2.6** halves, the steric constraints are gradually increased via a sequence involving: i) 1,3-dipolar cycloaddition to a five-membered thiadiazoline intermediate, ii) nitrogen elimination to form a three-membered episulfide **2.7,** and iii) sulfur extrusion to afford the desired alkene **2.4**.[20] Compound **2.4** was obtained as a mixture of four stereoisomers: (*M*)-*cis*, (*P*)-*cis*, (*M*)-*trans* and (*P*)-*trans*. The *cis*- and *trans*-isomers could be separated using flash column chromatography or HPLC and complete enantioresolution could be performed by chiral HPLC. The different isomers of **2.4** were characterized by mass spectroscopy, ^{1}H and ^{13}C NMR and UV-VIS and CD spectroscopy (*vide infra*).

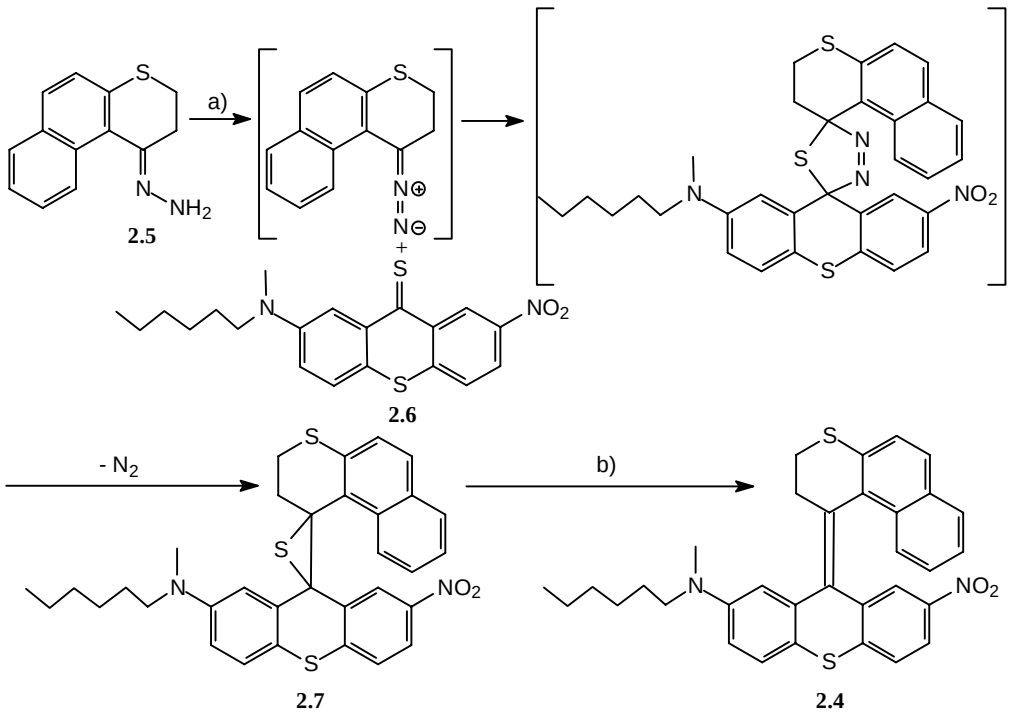

Scheme 2.6 The diazo-thioketone coupling illustrated for compound **2.4**: a) Ag_2O, $MgSO_4$, KOH/MeOH, CH_2Cl_2, -10 - 0°C, 85%, b) Cu, *p*-xylene, Δ, 79%.

The synthetic approach is based on the synthesis of the parent compound **2.2**, which started from (N,N)-dimethylaniline where the dimethylamine donor substituent is already present. The synthesis of compound **2.4** started with (N,N)-hexylmethylaniline **2.10**, readily obtained by a two stage reductive amination of caproic acid chloride (hexanoyl chloride) with N-methylaniline **2.8** (Scheme 2.7). From (N,N)-dialkylaniline **2.10**, the synthesis of **2.4** followed exactly the same 5 synthetic steps as for the synthesis of compound **2.2** to provide the desired donor-acceptor substituted thioketone lower half **2.6** used in the subsequent coupling reaction. The upper half hydrazone **2.5** is the same as the one used for compound **2.2**. Although for the formation of **2.4**, or any particular donor-acceptor switch, this synthetic strategy is as efficient as any other strategy one can immediately see the shortcomings of such a linear procedure when a variety of donor-acceptor substituted compounds has to be synthesized. It is therefore preferred to have a simple functionalization reaction late in the synthetic route as to have a somewhat convergent scheme to allow the easy preparation of a variety (a small library) of different chiroptical molecular switches. Mainly because due to the complicated nature of the exact photophysics involved in switching it is hard to predict beforehand which particular donor-acceptor switch will show the desired properties. Of course, an alternative strategy can be exploited using N-methylaniline as a starting compound. In each stage of the synthesis one can introduce, for example, by reductive amination with an aldehyde or acid, the desired functionality, such as a solubilizing group. This method has at least two major drawbacks; one is that the secondary amine moiety is rather sensitive and might cause several side reactions. A second drawback is that in this case only one of the substituents on the nitrogen center can be functionalized to obtain the

properties desired for a certain application. Therefore an alternative route using a palladium-catalyzed aromatic substitution reaction was investigated.

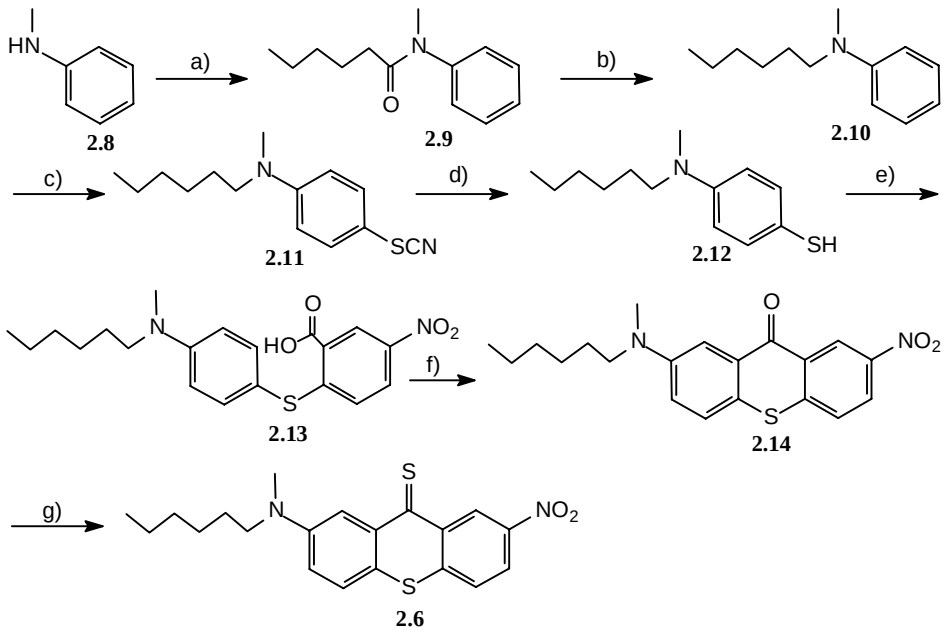

Scheme 2.7 Formation of thioketone **2.6** in a linear approach towards compound **2.4**: a) hexanoyl chloride, 86%, b) BH_3 / THF, Δ, 77%, c) KSCN, AcOH, Br_2, 86%, d) Na_2S, NaOH, EtOH, Δ, yield not determined, e) 2-chloro-5-nitro benzoic acid, KOH, EtOH, Δ, 94% (over two steps), f) polyphosphoric acid, 130°C, 56%, g) Lawesson's reagent, toluene, Δ, 73%.

The palladium-catalyzed amination of aryl halides has been extensively studied in recent years. Especially Buchwald *et al.* have published numerous examples of successful arene-substitutions using different amines, aryl halides and palladium catalysts, by which the scope of this reaction has been established.[21] Previous attempts, however, to functionalize aromatic halides with amine-substituents in the synthesis of chiroptical molecular switches failed due to low yields.[22] In the literature since then several modifications of the general amination reaction emerged rapidly, making it an even more versatile method. Especially the coupling of secondary amines to aromatic compounds bearing a bromo- or chloro-substituent provides good results. These reactions include different types of aromatic compounds with both electron-donating as well as electron-withdrawing substituents and commonly employ BINAP as a ligand and $Pd_2(dba)_3$ as a catalyst. The catalytic cycle where a Pd(0) species is proposed to be the active catalyst involves an oxidative addition of the aryl halide,[23] coordination and deprotonation of the amine and finally reductive elimination[24] of the N-aryl product (Scheme 2.8).

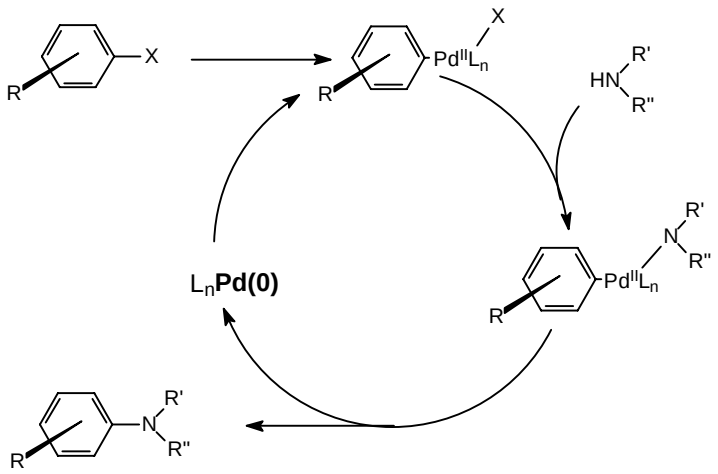

Scheme 2.8 Catalytic cycle for Pd-catalyzed amination of arylhalides (adapted from ref. 21).

A retrosynthetic analysis of donor-acceptor substituted molecular switches bearing a nitro electron acceptor substituent at the 7-position and a variable amino-based electron donating substituent at the 2-position is shown in Scheme 2.9. Although several retrosynthetic pathways can be envisioned, the bromo-substituted compound **2.15** would be the ideal synthon. Introduction of the donor substituent in compound **2.15**, that is the final stage of the switch synthesis, would offer an elegant and direct way to a variety of donor-acceptor substituted switches. The amination of **2.15** proved to be successful for a number of amine donors (Figure 2.3).

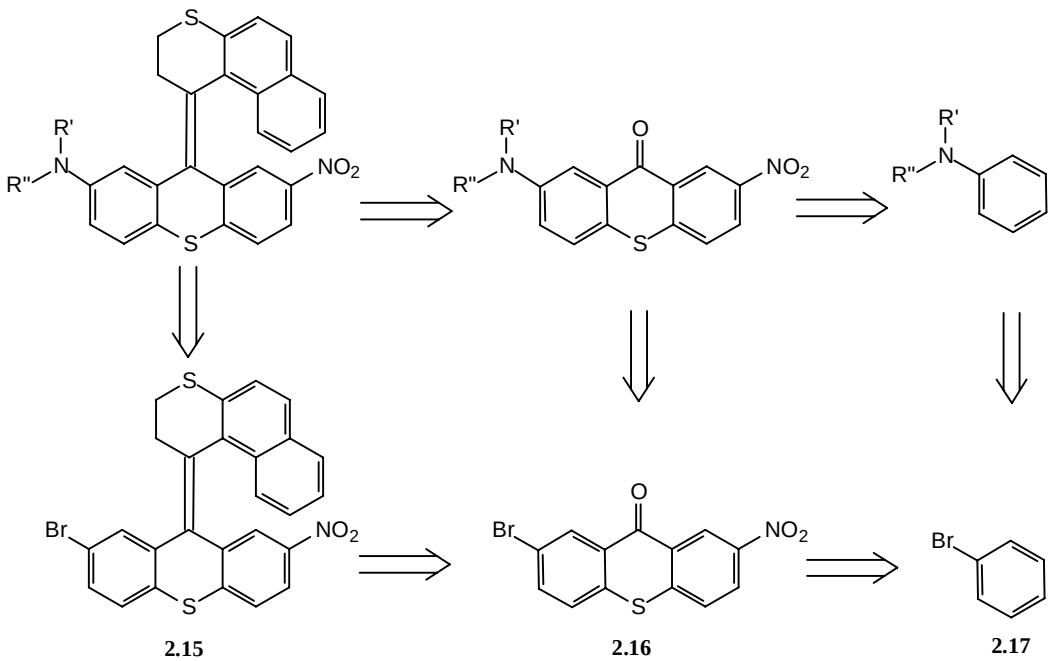

Scheme 2.9 Retrosynthetic analysis of a donor-acceptor switch synthesized via amination of an aryl halide.

The introduction of the linear aliphatic secondary amine, *n*-hexylmethylamine provided compound **2.4**. Also a cyclic amine ((*S*)-2-methoxymethylpyrrolidine) and an aromatic secondary amine (N-methylaniline) were introduced successfully leading to compounds **2.18** (whose synthesis and switching properties are described in Chapter 5) and **2.19**. The switching properties of the latter compound are described below. In the palladium catalyzed aminations $Pd_2(dba)_3$ was employed as the palladium source and BINAP as a ligand with toluene as the solvent (Scheme 2.10). The yields are 58 - 100%.

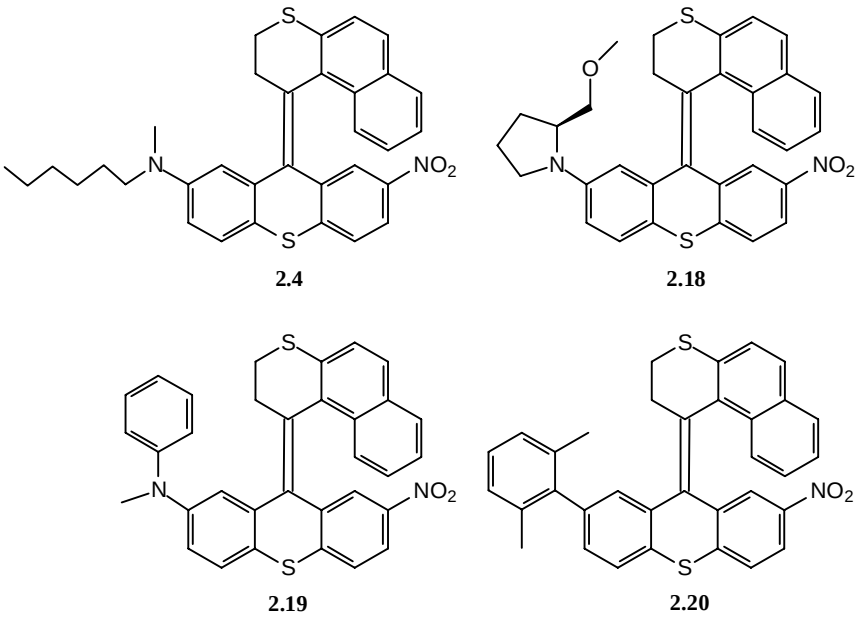

Figure 2.3 Novel molecular switches synthesized in one step from bromo compound **2.15**.

Next to the possibility of amine substitution a whole range of coupling reactions starting from aryl bromines are known. In an approach to develop a switchable molecular rotor (compound **1.19**, Chapter 1) a bromine-substituted lower half was already successfully used in a Suzuki coupling reaction. A Suzuki coupling, employing xylyl boronic acid was also successfully performed on compound **2.15** resulting directly in the new molecular rotor system **2.20** in 67% yield (Figure 2.3, Scheme 2.10). The dynamic and photophysical properties of this rotor compound are currently under investigation.

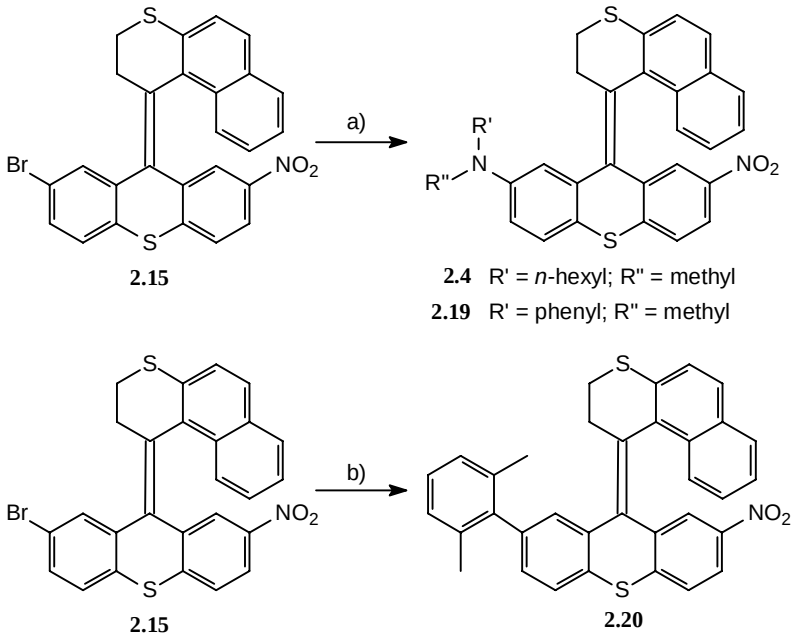

Scheme 2.10 Functionalization reactions of bromo-substituted synthon **2.15**, using palladium catalyzed amination: a) $Pd_2(dba)_3$, BINAP, NaOtBu, toluene, 80°C, yield: **2.4** quantitative, **2.18**: 58%, **2.19**: 87% and b) Suzuki coupling: $Pd(PPh_3)_4$, DME, $Ba(OH)_2 \cdot 8H_2O$, H_2O, xylyl boronic acid, 67%.

The synthesis of bromo-substituted overcrowded alkene **2.15** was performed via an approach similar to the one presented in Schemes 2.6 and 2.7. Starting from commercially available *p*-bromothiophenol (**2.21**) and 2-chloro-5-nitrobenzoic acid the lower half thioketone **2.23** was obtained in three steps (Scheme 2.11). Via a diazo-thioketone coupling with the generally used upper half hydrazone **2.5** the desired episulfide was formed which after desulfurization resulted in compound **2.15**.

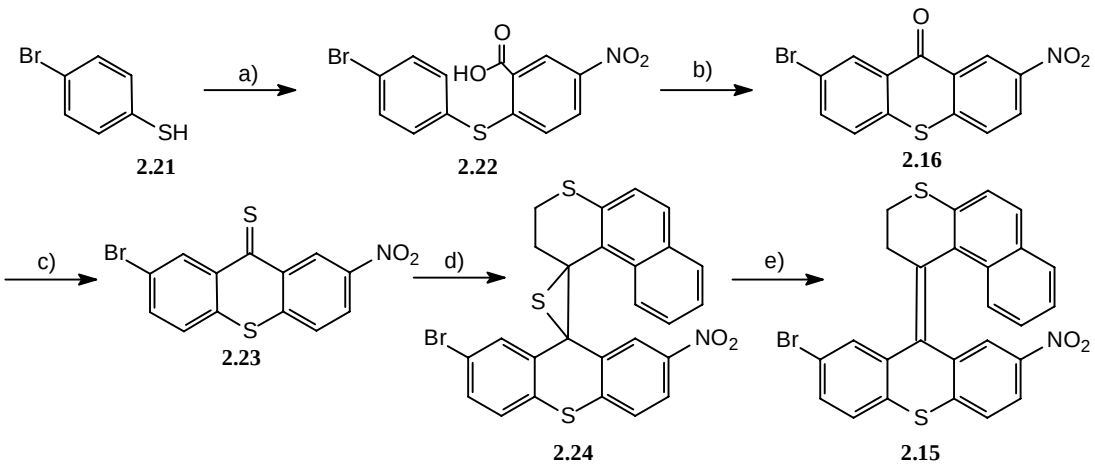

Scheme 2.11 Synthesis of bromo-substituted synthon **2.15**: a) 2-chloro-5-nitro benzoic acid, $NaHCO_3$, EtOH, Δ, b) sulfuric acid, 100°C, 95%, c) P_2S_5, toluene, Δ, 76%, d) Ag_2O, $MgSO_4$, KOH/MeOH, CH_2Cl_2, -10 - 0°C, 60%, e) Ph_3P, toluene, Δ, 97%.

In conclusion, using a late functionalization approach we now have direct synthetic access to a variety of donor-acceptor substituted switches by using different amines in the substitution reaction. For one example it was shown that other functionalized switches could be directly synthesized using the bromo-substituted synthon **2.15**. The new functionalization method allows the possibility of using enantiomerically pure **2.15** obtained by chiral HPLC resolution as a chiral synthon and, provided light and high temperatures are excluded, in a single step enantiomerically pure functionalized switches are obtained via the catalytic coupling reaction. HPLC resolution of both the *cis*- and *trans*-isomers of **2.15** was shown to be feasible where an analytical Chiralcel OD column showed nearly baseline separated peaks upon elution with *n*-heptane : isopropanol 99.5 : 0.5. Irradiation of a mixture of the four isomers of **2.15** did not lead to any change in UV-VIS absorption pattern while analysis of the diode-array signal obtained from the HPLC system showed substantial absorption differences between *cis*- and *trans*-**2.15**. This indicates the absence of *cis*-*trans* isomerization. This feature was also found for a similar fluoro-substituted chiroptical switch and can most likely be assigned to the electronic nature of the halogen substituent. Note that in **2.15** two electron-acceptor substituents are present in the lower half. This means that **2.15** is a photostable resolvable synthon for a variety of different functionalized switches. Furthermore, the presented method can be extended in several ways by employing different bromo-substituted molecular switches as synthons, which can bear a whole range of different substituents at different positions and furthermore the position of the bromine might be varied. Of course, in all cases reaction conditions have to be optimized. In this way it should also be readily possible to use a similar technique for a (combinatorial-like) synthesis of differently substituted variants of the second-generation motors discussed in Chapter 7 of this thesis.

2.4 Photophysical Properties of New Donor-Acceptor Systems

2.4.1 n-Hexyl Functionalized Donor-Acceptor Switch

Donor-acceptor compound **2.4** was designed to increase the solubility without interfering with the switching efficiency. The aim was to develop a novel helically shaped sterically overcrowded alkene with improved liquid crystalline compatibility, where switching between two pseudoenantiomeric forms was still efficient. Scheme 2.12 shows the envisioned switching scheme of (*M*)-*cis*-**2.4** and (*P*)-*trans*-**2.4**. After synthesis either via the linear as well as the convergent route, separate crystallization of racemic *cis*-**2.4** and *trans*-**2.4** from dichloromethane by slow evaporation under an *n*-hexane saturated atmosphere yielded crystals suitable for X-ray analysis (Figure 2.4). Both *cis*-**2.4** and *trans*-**2.4** crystallize in a triclinic unit cell, where both the (*M*)-enantiomer and the (*P*)-enantiomer are present in one unit-cell of space group P_1^-. The X-ray structures for (*M*)-*cis*-**2.4** and (*P*)-*trans*-**2.4** are depicted in Figure 2.4 where the carbon atoms of the molecular skeletons are numbered separately for the upper and lower half for convenience.

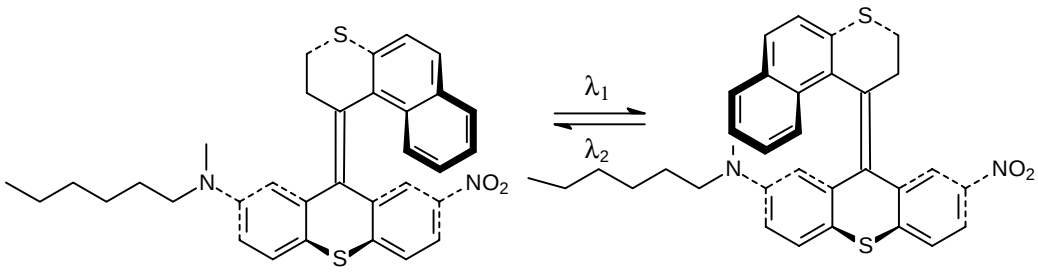

Scheme 2.12 Switching of an *n*-hexyl functionalized donor-acceptor switch.

The X-ray structure clearly shows the helical geometry for both pseudoenantiomers of this system. In the antifolded structure upper and lower halves of the molecule are tilted up and down, respectively relative to the plane of the central double bond. The upper heterocyclic rings adopt a twisted boat conformation in both cases, which is comparable to parent compound **2.2**.

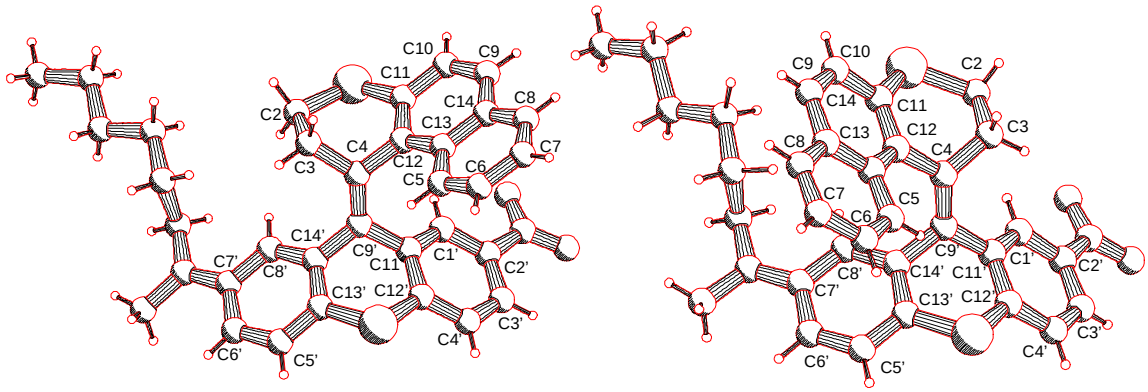

Figure 2.4 ORTEP plot of X-ray structure of (*M*)-*cis*-**2.4** (left) and (*P*)-*trans*-**2.4** (right) obtained from racemic crystals (the unit cell contains both (*M*)- and (*P*)-enantiomers in each case of which only one enantiomer is shown).

The central double bond has a length of 1.347 Å for *cis*-**2.4** and 1.357 Å for *trans*-**2.4**, values characteristic for a normal olefinic bond and comparable to the value of 1.353 Å found for *cis*-**2.2**. The helical geometry is best described by the torsion angles in the vicinity of the central double bond. For (*M*)-*cis*-**2.4** the dihedral angles C12-C4-C9'-C11' and C3-C4-C9'-C14' are -2.92° and -7.23°, respectively, clearly indicating substantial folding around the central double bond. For (*M*)-*cis*-**2.2** these angles were determined to be 0.4° and -5.4°, respectively indicating significantly less folding in the structure. The values of (*P*)-*trans*-**2.4** were determined to be 0.55° and 6.65° for C12-C4-C9'-C14' and C3-C4-C9'-C11' with clearly less folding than the *cis*-isomers. This is underlined by the angle of the upper half aromatic moiety (C5-C14) relative to the lower half aromatic moiety directly adjacent to this upper half (the nitro-arene for the *cis*-isomer (C1'-C2'-C3'-C4'- C12'-C11') and the dialkylamine-

arene (C5'-C6'-C7'-C8'- C14'-C13') for the *trans*-isomer) which was 49.4° for the *trans*-isomer and 54.4° for the *cis*-isomer. The folded structure of the lower halves for both compounds is reflected in the dihedral angles C9'-C14'-C13'-S and C9'-C11'-C12'-S which were determined to be -0.17° and -0.30° for (*M*)-*cis*-**2.4** and -2.5° and 1.2° for (*P*)-*trans*-**2.4**. The *trans*-isomer therefore shows significantly larger folding although this is only slightly reflected in the angles between the two aromatic rings in the bend lower half which were determined to be 138.4° for the *cis*-isomer and 138.1° for the *trans*-isomer. To graphically illustrate these differences the X-ray structures of (*M*)-*cis*-**2.4** and (*M*)-*trans*-**2.4** (the exact mirror image of the discussed structure of (*P*)-*trans*-**2.4**) were overlain (Figure 2.5). Although there are subtle differences between the two forms, this is the first direct observation of the pseudoenantiomeric relationship of two forms of a chiroptical molecular switch based on a sterically overcrowded alkene. The racemization barrier ($\Delta G^{\ddagger}$) for the (*M*)-*trans*-**2.4** was determined to be 118.4 kJ mol^{-1} in toluene solution at 80°C by CD spectroscopy. This value is comparable though lower than the value found for *trans*-**2.2**, which was 122.2 kJ mol^{-1}. For the *cis*-isomer in the same way a slightly higher racemization barrier of 124.6 kJ mol^{-1} was determined.

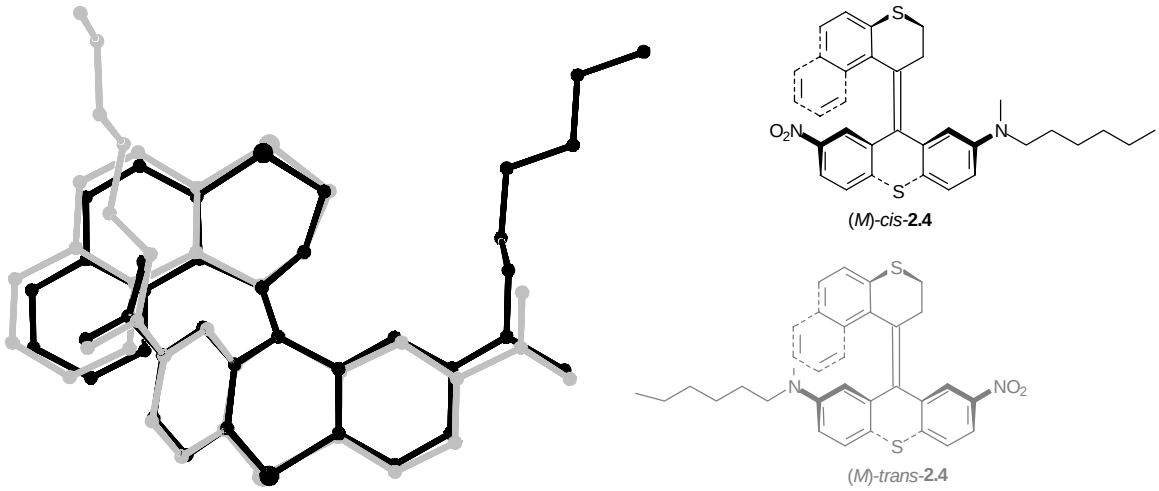

Figure 2.5 Direct proof for a pseudoenantiomeric relationship based on overlain X-ray structures of (*M*)-*cis*-**2.4** (black) and (*M*)-*trans*-**2.4** (gray).

Due to the helical structure of compounds **2.4** strong CD effects in *n*-hexane solution are observed for both isomers of the switching system (Figure 2.6 bottom). As expected the spectral features are similar to those of compound **2.2**. The pseudoenantiomeric nature of the (*M*)-*cis*-**2.4** and (*P*)-*trans*-**2.4** isomers is clearly reflected in the CD spectra. In *n*-hexane solution similar UV-VIS spectra for **2.2** and **2.4** are also found with a slight red shift for **2.4**. Distinct differences between the absorptions of *cis*-**2.4** and *trans*-**2.4** are observed throughout the entire absorption spectra (Figure 2.6 top). The *cis*-isomer shows a distinct UV-VIS band with a maximum at 373 nm whereas the *trans*-isomer shows a less distinct broadened band with a shoulder at the high wavelength side without a clear maximum. This broadened band for the *trans*-isomers results in a bathochromic shift of the maximum wavelength. The *cis*-isomer shows absorption up to about 455 nm the long wavelength absorption band of the *trans*-isomer is stretched to about 468 nm. This effect (which is also present in parent

compound **2.2** but to a lesser extent) can be used for efficient switching since at wavelengths where only one of the forms of the bistable system shows absorption, theoretically switching with 100% efficiency should be possible.

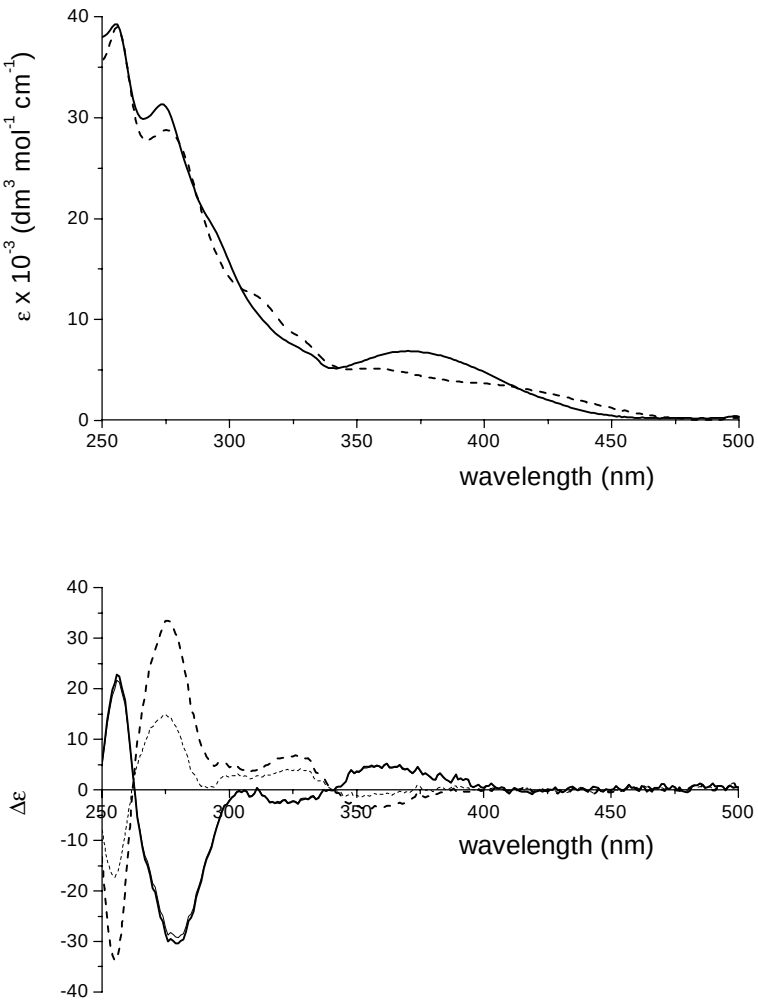

Figure 2.6 UV-VIS (top) and CD spectra (bottom) of (*M*)-*cis*-**2.4** and (*P*)-*trans*-**2.4**. The solid curves correspond to (*M*)-*cis*-**2.4** and the dashed curves to (*P*)-*trans*-**2.4**. Also depicted in the lower graph are the CD spectra obtained for the two photostationary states 465 nm (thin solid curve) and 380 nm (thin dashed curve).

The actual factor that governs the switching efficiency is the ratio of extinction coefficients plotted in Figure 2.7. It is immediately evident that the most efficient switching wavelengths in *n*-hexane are 380 nm and about 455 nm. As noted, *n*-hexane was already shown to be the most efficient solvent for this type of systems. Furthermore, it should be emphasized that upon increasing the irradiation wavelength the time to reach the photoequilibrium will increase due to decreasing absorption.

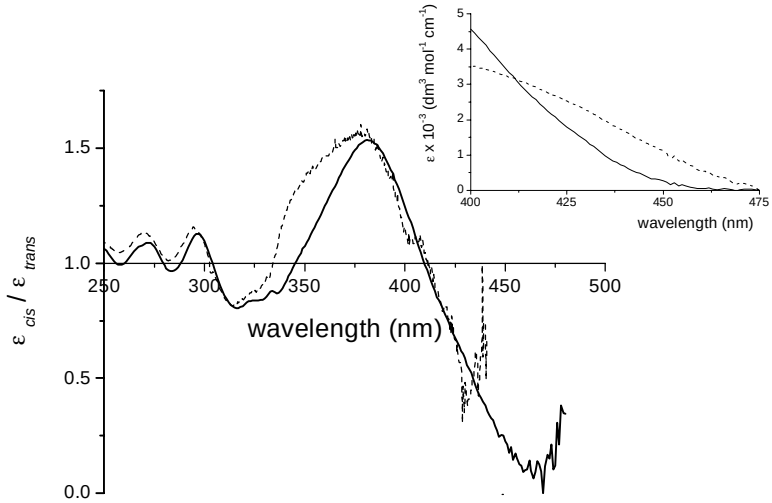

Figure 2.7 Ratio of extinction coefficients for the *cis*-and *trans*-form of compound **2.4** (solid curve, the ratio found for compound **2.2** is given as a comparison (dashed curve)). The inset shows the red-end of the absorption spectrum for the *cis*- (solid) and *trans*- (dashed) form of **2.4**.

Switching experiments were mainly performed on resolved enantiomerically pure *trans*-isomers since HPLC resolution of *trans*-**2.4** proved to be facilitated considerably compared to the resolution of the *cis*-isomer. Actually using a Chiralcel OD column the first eluted fraction, when *n*-hexane or *n*-heptane / isopropanol mixtures are used as eluent, was assigned to be (*P*)-*trans* by ^{1}H NMR spectroscopy and by comparing the CD spectrum of this fraction with the CD spectra of the different isomers of compound **2.4**. The chemical shift of the N-methyl protons (δ 2.27 ppm) clearly indicates the *trans* orientation, whereas for *cis*-**2.4** the N-methyl proton absorptions are located at 3.02 ppm. Subsequently, (*P*)-*cis*-**2.4** and (*M*)-*cis*-**2.4** were eluted followed by (*M*)-*trans*-**2.4**. Starting from either enantiomerically pure or racemic *trans*-**2.4** in *n*-hexane solution irradiation at the most efficient wavelength of 380 nm resulted in the formation of a photostationary state consisting of 70% *trans*-**2.4** and 30% *cis*-**2.4**. This corresponds to an efficiency equal to that for the parent compound **2.2** for the *trans* photostationary state. Changing the wavelength of irradiation only had a decreasing effect on the efficiency that is a decreased diastereomeric excess was obtained at the photostationary states. Subsequent irradiation at 455 nm resulted in the formation of a photostationary state consisting of 95% *cis*-**2.4** and 5% *trans*-**2.4**. This switching process is reversible and for three consecutive *trans*→*cis*→*trans* isomerizations no change in photoequilibria or fatigue was observed. Extrapolating the results found for compound **2.2** it can be assumed that also for this compound repeated isomerizations would not be a problem.

Increasing the wavelength of irradiation to 460 nm and subsequently to 465 nm resulted in even more efficient photostationary states of 97 : 3 and 98 : 2 diastereomeric ratio of *cis*-**2.4** to *trans*-**2.4**, respectively, as determined by HPLC. Considering the errors in HPLC determination, this system thus shows nearly quantitative switching to a *cis* photostationary state, due to the fact that at the highest wavelength region only the *trans*-isomer shows UV-

VIS absorption. Irradiation at the isosbestic point (304.5 nm) resulted in a near pseudoracemic photostationary state of 51% *cis*-**2.4** and 49% *trans*-**2.4** indicating comparable quantum yields for the photoisomerization in both directions. With a switching efficiency towards the *trans*-isomer at 380 nm (*cis* : *trans* ratio: 30 : 70) being equal to that of the parent donor-acceptor compound **2.2** we have developed here the most efficient chiroptical molecular switch thus far (Scheme 2.13).

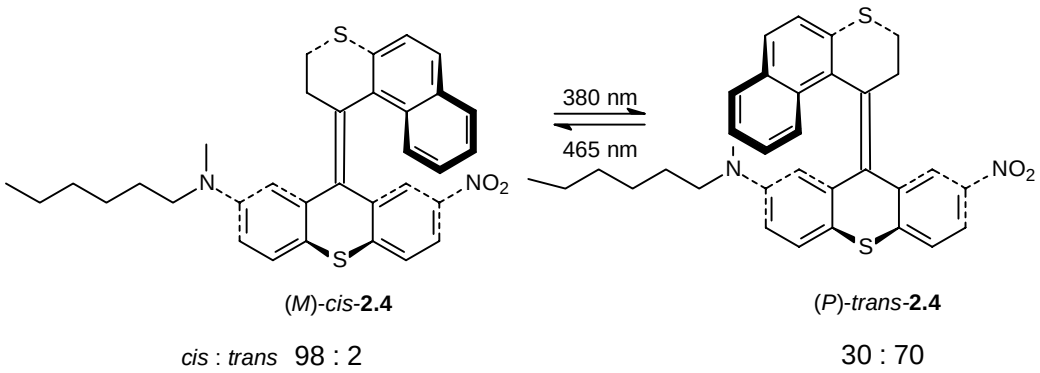

Scheme 2.13 Highly efficient chiroptical molecular switch **2.4**.

The increased efficiency is caused by a slight bathochomic shift of the UV-VIS curve of the *trans*-isomer relative to the *cis*-isomer (inset Figure 2.7). Although this is only a minor effect it allows irradiation at the red-edge of the spectrum to almost exclusively excite the *trans*-isomer resulting in a near quantitative switching to the *cis* photostationary state. The ratio of the two extinction coefficients is the determining factor here. Figure 2.7 shows a direct comparison of the ratio of the absorption of *cis*- and *trans*-isomers found for compound **2.2**[25] and **2.4**.

2.4.2 Rapid Screening of Switching Efficiencies

The development of a fast method for the synthesis of a variety of donor-acceptor switches or even differently functionalized systems calls for a compatible fast screening process for switching efficiencies. Where in the past, and illustrated for the previous example **2.4** discussed in the previous paragraph, actual switching experiments were preceded by tedious and time-consuming preparative HPLC resolution steps this is not necessary in the determination of switching efficiencies. In some cases even actual switching experiments were abandoned when resolution proved to be too difficult, but not even a separation of *cis*- and *trans*-isomers is required for efficiency measurements.

For compound **2.19**, in which the donor substituent is a methylphenylamine and where the additional phenyl chromophore might have considerable effect on the photochemical behavior, the switching efficiencies were determined without resolution. A UV-VIS absorption curve in *n*-hexane was determined for a mixture of the four stereoisomers (*M*)-*cis*, (*P*)-*cis*, (*M*)-*trans* and (*P*)-*trans*-**2.19**, in unknown ratios (a small detail is depicted in Figure 2.8). In principle even contaminated samples can be used as long as the contamination is not photoactive. This mixture was irradiated with 365 nm light (the wavelength here is chosen at random with the only requirement that the system actually absorbs at this wavelength)

inducing two photoisomerization processes. Photoisomerizations between (*M*)-*cis*-**2.19** and (*P*)-*trans*-**2.19** as well as between (*P*)-*cis*-**2.19** and (*M*)-*trans*-**2.19** are simultaneously induced. After a short irradiation period (5 min), a second UV-VIS spectrum is taken and from the ratio of the two one can immediately determine the most efficient wavelengths for switching (here: 379 and 446 nm) as well as the isosbestic points (here: 343 (not shown) and 398 nm) which are necessary to determine the relative ratios by HPLC diode array detection. It should be noted that since the depicted ratio is the ratio between the initial UV-VIS curve and the UV-VIS curve obtained after short irradiation, this cannot be quantitatively compared to the ratios of extinction coefficients of two pseudoenantiomers as depicted in Figure 2.7. It is clearly visible that the effect found for compound **2.4**, where the absorption curve of one of the two switch forms has shifted to higher wavelength values, is absent here.

Subsequently the mixture was irradiated at 379 nm monitoring the UV-VIS spectra in time to ensure full photoequilibration. Monitoring the photochemical process at either one of the isosbestic points by analytical HPLC (a Chiralcel OD column was used for **2.19** and *n*-heptane : isopropanol 95 : 5 as an eluent) gave a *trans* to *cis* ratio of 66 : 34 at this photostationary state. *Cis*- and *trans*-isomers of **2.19** are assigned by comparing UV-VIS absorptions with those of compounds **2.2** and **2.4**. The fraction with the most distinct absorption around 370 nm was assigned *cis*-**2.19** whereas the fraction with the most red-shifted shoulder was assigned *trans*-**2.19**. Irradiation at 446 nm resulted in a second photostationary state with a *cis* : *trans* ratio of 95 : 5.

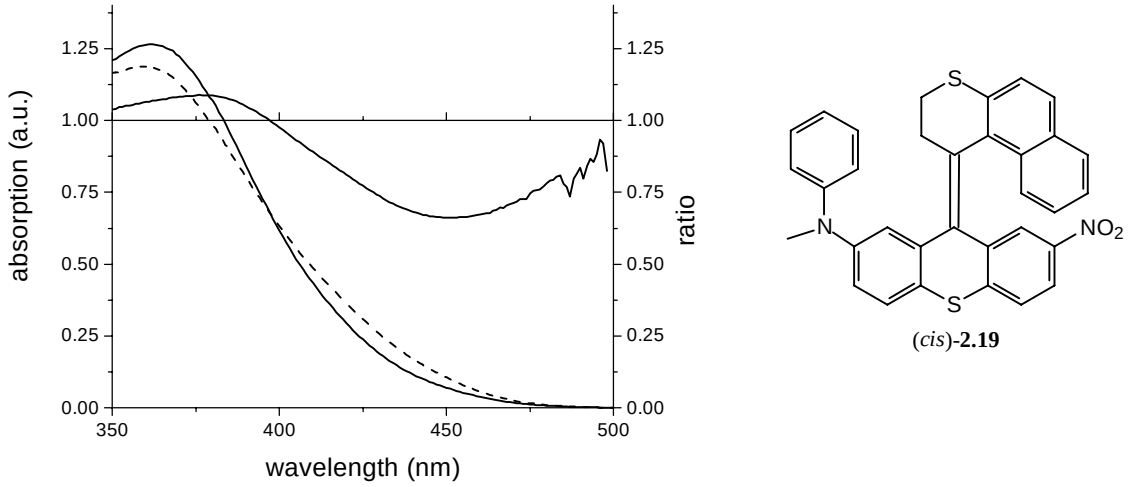

Figure 2.8 UV-VIS absorption of compound **2.19** (mixture of four isomers in *n*-hexane; *cis*-**2.19** depicted) without prior resolution or irradiation (solid) and after 5 min of irradiation at 365 nm (dashed), plotted together with their ratio ($abs(t_0)$ / $abs(t_5)$).

Although **2.19** constitutes a relatively efficient switch, the extra chromophore does not have a substantial positive influence. It should be noted that the additional phenyl group has a large influence on the HPLC separation of the four stereoisomers. Using again a Chiralcel OD column with *n*-hexane : isopropanol as eluent, the order of elution has changed. First the two *trans*-enantiomers are eluted and consecutively the two *cis*-enantiomers and near baseline

separation of all four forms is achieved. An additional advantage of this type of system is that its properties can be tuned by using differently substituted anilines in the coupling reaction. No resolution and chiroptical measurements were performed so far, however, if desired one can still decide to revert to the original resolution and actual chiral switching.

2.4.3 Simplified Donor- and Acceptor-Only Systems

In order to get information on the actual necessity that both an electron-donor and an electron-acceptor moiety are present in the same molecule to induce efficient switching, the acceptor-only nitro-substituted and donor-only dimethylamine-substituted switches **2.26** and **2.28**, respectively, were synthesized using a linear synthetic approach (Scheme 2.14).

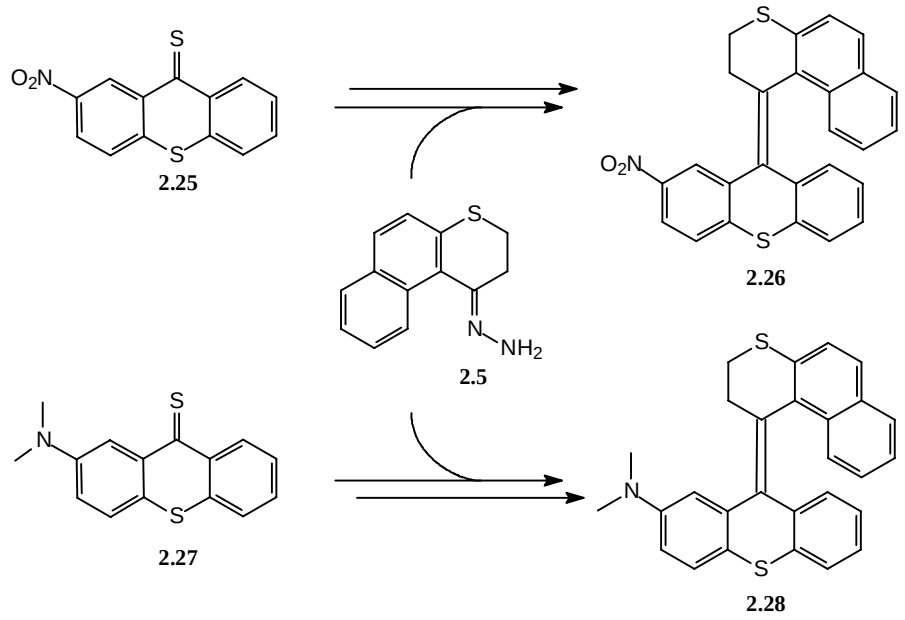

Scheme 2.14 Simplified analogues of the donor-acceptor switches, acceptor-only compound **2.26** and donor-only compound **2.28**.

Using a similar rapid switching procedure as described in section 2.4.2, the relative switching efficiencies of **2.26** and **2.28** in *n*-hexane were determined. Most efficient photoswitching for acceptor substituted switch **2.26** was observed upon irradiation at 324 and 402 nm. These wavelengths are considerably blue-shifted compared to the donor-acceptor switches due to the absence of a charge transfer absorption band. At 324 nm a diastereomeric ratio of 55 : 45 was observed in favor of the *trans*-isomer (assignment based on UV spectra) and at 402 nm a diastereomeric ratio of 77 : 23 was observed in favor of the *cis*-isomer (ratios were determined by HPLC analysis). For donor compound **2.28** most efficient switching was found at 370 and 407 nm; again the optimized wavelengths for **2.28** are blue shifted compared to those of the donor-acceptor compounds. At 370 nm a diastereomeric ratio of 67 : 33 was observed in favor of the *cis*-isomer. This was confirmed by NMR spectroscopy where *cis*- and *trans*-isomers can be easily assigned based on the differences in chemical shift of the N-methyl protons (2.25 ppm for *cis*-**2.28** and 3.02 ppm for *trans*-**2.28**). Note that in the case of **2.28**, in the isomer that is assigned as *cis* the upper half of the molecule is on the same side as the dimethylamine group in the lower half. As such it should be compared with the *trans*-

isomers in the donor-acceptor systems presented earlier (compounds **2.2**, **2.4**, and **2.19**). At 407 nm a diastereomeric ratio of 72 : 28 was observed in favor of the *trans*-isomer.

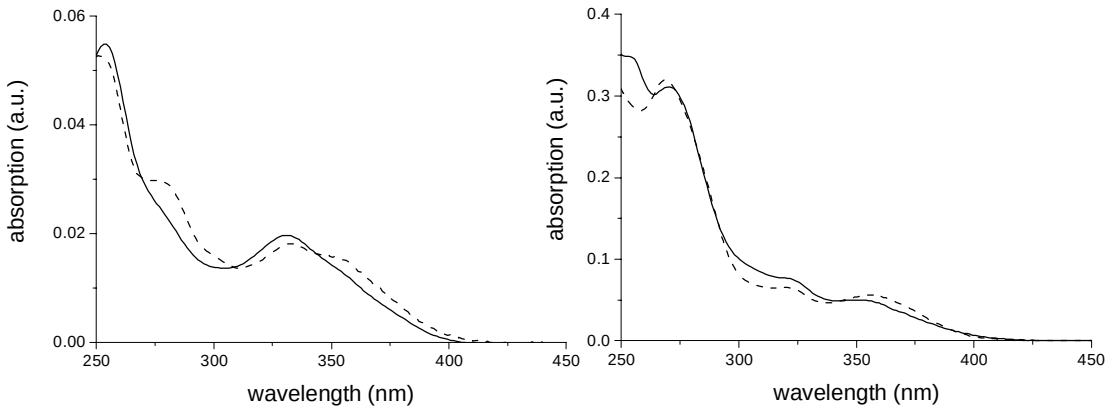

Figure 2.9 UV-VIS absorption spectra for acceptor switch **2.26** (left) and donor switch **2.28** (right). Solid curves indicate the *cis*-isomers and dashed curves indicate *trans*-isomers obtained from diode array PDA detection directly after chiral HPLC separation.

A first conclusion that can be drawn for both compounds **2.26** and **2.28** is that switching selectivities are lower than for the donor-acceptor systems. For fair comparison compound **2.2** should be used. Both for irradiation at shorter wavelength (which corresponds to *trans* photostationary states for compounds **2.2** and **2.26** and to a *cis* photostationary state for compound **2.28**) as well as irradiation at longer wavelengths, selectivities decreased considerably. Scaling the UV-VIS absorption spectra of the *cis*- and *trans*-isomers of **2.26** and **2.28** obtained directly from diode array detection after chiral HPLC separation by equalizing at the isosbestic points roughly give UV-VIS spectra in the HPLC eluent approximated at equal concentration (Figure 2.9).

For the donor-acceptor switches **2.2** and **2.4** the far edge of the UV-VIS absorption of the *trans*-isomers was red-shifted compared to the *cis*-isomers. This resulted in selective switching towards the *cis*-isomers at 435 and 465 nm, respectively, for **2.2** and **2.4**. Comparing the UV-VIS spectra of compounds **2.26** and **2.28** it is evident that this red-shift of the UV-VIS spectrum has to be attributed to the presence of the acceptor substituent, since similar behavior is observed only for the acceptor substituted compound **2.26**. *Cis*-**2.26** showed UV-VIS absorptions up to about 405 nm while for *trans*-**2.26** the maximum absorption wavelength was shown to be approximately 425 nm. For donor compound **2.28** UV-VIS absorptions up to about 410 nm are observed for both *cis*- and *trans*-isomers. Differences in absorption around 365 nm (for **2.2**, Figure 2.1) and 380 nm (for **2.4**, Figure 2.6 and 2.7) can mainly be assigned to the presence of the electron-donor substituent since similar behavior is observed for the donor substituted compound **2.28** around 310 nm. In accordance with these observations, the acceptor-only compound **2.26** shows higher efficiency at the higher wavelength photostationary state (with a diastereomeric excess of 54% compared to a value of 44% for **2.28)**. The donor-only compound **2.28** shows higher

efficiency at the lower wavelength photostationary state (with a diastereomeric excess of 34% compared to a value of 10% found for **2.26**). This leads to a careful conclusion that indeed a combination of both an electron-donor and an electron-acceptor substituent will lead to efficient reversible photoswitches. Since the lower wavelength photostationary state in the donor-acceptor switches still leaves considerable room for enhanced selectivity, future improvements on the switching selectivities are most likely expected by varying the properties of the donor substituent on the molecular skeleton. For this goal now a very efficient synthetic strategy has been developed.

2.5 Conclusion

The newly designed donor-acceptor switch **2.4** proved to be the most efficient molecular switch based on sterically overcrowded alkenes, developed thus far. Selectivities in the photostationary states with *cis*-**2.4** : *trans*-**2.4** ratios of 30 : 70 (380 nm) and 98 : 2 (465 nm) are reached in *n*-hexane. Further improvement on the selectivity towards the *trans* photostationary state is still a main objective for further research. Studies on simplified donor- and acceptor-only systems **2.26** and **2.28** showed that this improvement should be focussed primarily on changing the donor properties of the molecular system. This can be done efficiently in the synthetic route by a late amination step of a bromo-substituted precursor of the molecular switches also introduced in this chapter.

Essential in the further development towards actual molecular devices is the retention of properties in a larger array or organized environment. All aspects discussed in this chapter, although highly illustrative with respect to the molecular processes involved, relate to measurements in solution. Application requires a more processable medium where the properties of the molecular system are retained or even amplified. Liquid crystalline host materials already widely applied in display technology, offer one approach that will be discussed in the following chapter.

2.6 Experimental Section

General Remarks

^{1}H NMR spectra were recorded on a Varian VXR-300 (300 MHz) or a Varian Unity Plus Varian-500 (500 MHz). ^{13}C NMR spectra were recorded on a Varian VXR-300 (75 MHz) or a Varian Unity Plus Varian-500 (125 MHz). Unless stated otherwise, ^{1}H NMR data are obtained at 300 MHz and ^{13}C NMR data are obtained at 75 MHz measurement, both in $CDCl_3$. Chemical shifts are denoted in δ-unit (ppm) relative to $CDCl_3$, and the NMR data of C_2-symmetrical compounds are listed for half a molecule. The splitting patterns are designated as follows: s (singlet), d (doublet), t (triplet), q (quartet), m (multiplet) and b (broad) for ^{1}H NMR. For ^{13}C NMR the carbon atoms are assigned as t (primary carbon), d (secondary carbon), s (tertiary carbon) and q (quaternary carbon). CD spectra were recorded on a JASCO J-715 spectropolarimeter and UV measurements were performed on a Hewlett-Packard HP 8453 FT Spectrophotometer using UVASOL grade solvents (Merck). MS spectra were obtained with a Jeol JMS-600 spectrometer by Mr. A. Kieviet. Column chromatography was performed on silica gel (Aldrich 60, 230-400 mesh). HPLC analyses were performed on a Waters

HPLC system equipped of a 600E solvent delivery system and a 996 Photodiode Array Detector. Preparative HPLC was performed by Mr. M. van Gelder on a preparative Gilson HPLC system consisting of a 231XL sampling injector, a 306 (10SC) pump, an 811C dynamic mixer, a 805 manometric module, with a 119 UV-VIS detector and a 202 fraction collector, using the (chiral) columns as mentioned. Elution speed was 1 ml min^{-1}, unless stated otherwise. Elemental analyses were performed in our microanalytical department by Mr. J. Hommes. X-ray diffraction measurements were performed by Drs. A. Meetsma in our laboratory employing a Bruker SMART APEX CCD diffractometer. If necessary, solvents were distilled and dried before use by standard methods. Reagents and starting materials were used as obtained from Aldrich, Acros Chimica, Fluka or Merck.

Irradiation experiments.
Irradiations were performed with an 150 W Oriel Xe-lamp attached to an Oriel monochromator or a 180 W Oriel Hg-lamp adapted with a suitable Mercury line filter for 313, 365, 405 and 435 nm irradiations (typical bandwidth 10 nm). Photostationary states are ensured by monitoring composition changes in time by taking UV spectra at distinct intervals until no changes were observed. Ratios of the different forms of the molecular switches were determined by HPLC by monitoring at the isosbestic point or by NMR analysis. HPLC elution times and NMR details are denoted throughout the synthetic procedures.

2,3-Dihydro-1H-naphtho[2,1-b]thiopyran-1-one hydrazone (2.5).[18] Starting for 2-thionaphthol, via 3-(2-naphthylthio)-propiononitrile and 2,3-dihydro-1H-naphtho[2,1-b]thiopyran-1-one 2,3-dihydro-1H-naphtho[2,1-b]thiopyran-1-one hydrazone was synthesized. ^{1}H NMR δ 2.87 (s, 4H), 5.43 (bs, 2H), 7.31 (d, *J* = 8.4 Hz, 1H), 7.37 (ddd, *J* = 8.1, 7.0, 1.1 Hz, 1H), 7.46 (ddd, J= 8.8, 7.0, 1.5 Hz, 1H), 7.58 (d, *J* = 8.4 Hz, 1H), 7.72 (dd, *J* = 8.1, 1.5 Hz, 1H), 8.65 (d, *J* = 8.8 Hz, 1H). ^{13}C NMR δ 27.27 (t), 30.31 (t), 124.93 (d), 126.37 (d), 126.46 (d), 126.66 (d), 127.59 (d), 127.85 (d), 129.60 (s), 131.39 (s), 132.94 (s), 135.94 (s), 145.23 (s).

Hexanoyl chloride. To thionyl chloride (48 ml, 0.65 mol) was slowly added caproic acid (54 ml, 0.44 mol). The mixture was refluxed for half an hour and the acid chloride was collected by distillation at 151-153°C (55.0 g, 95%). ^{1}H NMR δ 0.34 (t, *J* = 6.3 Hz, 3H), 0.71 (m, 4H), 1.12 (m, 2H), 1.62 (bt, *J* = 6.6 Hz, 2H), 2.78 (s, 3H), 6.74 (bd, *J* = 7.5 Hz, 2H), 6.84 (bt, *J* =7.5 Hz, 1H), 6.95 (bt, *J* = 7.5 Hz, 2H). ^{13}C NMR δ 13.06 (t), 21.58 (d), 24.37 (d), 30.62 (d), 33.13 (d), 36.29 (t), 121.22 (s), 126.53 (s), 126.79 (s), 128.76 (s), 128,91 (s), 143.59 (q), 171.83 (q).

***N*-methylhexanoylaniline (2.9)**. To *N*-methylaniline **2.8 (**32.2 ml, 300 mmol) was carefully added dropwise hexanoyl chloride (20.0 g, 150 mmol). After complete addition the reaction mixture was stirred for an additional hour and then diluted with water (200 ml). The product was extracted with water and washed with 10% HCl solution and water. After drying with sodium sulfate and evaporation of the solvent, *N*-methylhexoylaniline **2.9** (26.2 g, 86%) was obtained. ^{1}H NMR δ 0.34 (t, *J* = 6.3 Hz, 3H), 0.71 (m, 4H), 1.12 (m, 2H), 1.62 (bt, *J* = 6.6 Hz, 2H), 2.78 (s, 3H), 6.74 (bd, *J* = 7.5 Hz, 2H), 6.84 (bt, *J* =7.5 Hz, 1H), 6.95 (bt, *J* = 7.5 Hz, 2H). ^{13}C NMR δ 13.06 (t), 21.58 (d), 24.37 (d), 30.62 (d), 33.13 (d), 36.29 (t), 121.22 (s), 126.53 (s), 126.79 (s), 128.76 (s), 128,91 (s), 143.59 (q), 171.83 (q). HRMS calcd for $C_{13}H_{19}NO$: 205.14666, found: 205.14519.

***N*-Methylhexylaniline 2.10**. At a constant temperature of 0°C, a solution of *N*-methylhexanoylaniline **2.9** (6.16 g, 30 mmol) in THF (30 ml) was added to 1M BH_3 in THF (50 ml) in 30 min. After complete addition the reaction mixture was slowly heated and refluxed for 1 h. Consecutively, the

reaction mixture was cooled to room temperature and a 6M HCl solution (8 ml) was added dropwise. The THF was distilled off at atmospheric pressure and the residue was saturated with NaOH. Triple extraction with ether (50 ml) yielded, after drying and evaporation of the solvent *N*-methylhexylaniline **2.10** (4.41 g, 77%) as an oil which was further purified by Kugelrohr distillation (60°C, 0.02 mmHg). ^{1}H NMR δ 1.13 (bm, 3H), 1.54 (bs, 6H), 1.78 (bs, 2H), 3.11 (m, 3H), 3.46-3.52 (m, 2H), 6.86-6.92 (m, 3H), 7.40-7.47 (m, 2H). ^{13}C NMR δ 14.53 (t), 23.19 (d), 27.12 (d), 27.35 (d), 38.65 (t), 53.28 (d) 112.56 (s), 116.30 (s), 129.57 (t), 149.83 (q). HRMS calcd for $C_{13}H_{21}N$: 191.16739, found: 191.16777.

***N*-methylhexyl-4-thiocyanoaniline 2.11**. A solution of KSCN (5.32 g, 55 mmol) *N*-methylhexylaniline **2.10** (5.00 g, 26.1 mmol) in acetic acid (50 ml) was cooled to 10°C. While stirring this solution mechanically, a solution of Br_2 (4.2 g, 26.2 mmol) in acetic acid (5 ml) was slowly added keeping the temperature of the mixture at 10°C. After the addition was complete the mixture was poured into water (300 ml) and extracted with ether. After drying and evaporation *N*-methylhexyl-4-thiocyanoaniline **2.11** (5.57 g, 86%) was obtained. ^{1}H NMR δ 0.94 (bm, 3H), 1.33 (bs, 6H), 1.57 (bs, 2H), 2.95 (s, 3H), 3.29-3.34 (m, 2H), 6.64 (d, *J* = 8.7 Hz, 2H), 7.39 (d, *J* = 8.7 Hz, 2H). ^{13}C NMR δ 13.95 (t), 22.55 (d), 26.48 (d), 26.59 (d), 38.20 (t), 52.29 (d), 105.34 (q), 112.72 (s), 129.20 (q), 134.51 (t), 150.54 (q). HRMS calcd for $C_{14}H_{20}N_2S$: 248.13471, found: 248.13556.

4-(*N*-methylhexylamino)-thiophenol 2.12. To a solution of NaOH (3.3 g, 82.5 mmol) in dry ethanol (200 ml) under a N_2 atmosphere, were added $MgSO_4$ (3 g), $Na_2S{\cdot}5H_2O$ (15 g, 90 mmol) and *N*-methylhexyl-4-thiocyanoaniline **2.11** (16.8 g, 68 mmol). This mixture was refluxed for 4 h, filtered into a solution of NH_4Cl (9 g) in water (150 ml) and the resulting mixture was extracted twice with ether (100 ml). After drying and evaporation of the solvent the obtained thiophenol was used in the next step without purification and characterization due to the extreme oxidation sensitivity of the compound.

2-({4-[*N*-methylhexylamino]phenyl}sulfanyl)-5-nitrobenzoic acid 2.13. The crude 4-(*N*-methylhexylamino)-thiophenol was added to a solution of KOH (3.6 g) in dry ethanol (150 ml) whereupon 2-chloro-5-nitro benzoic acid (13.8 g, 69 mmol) was added and the reaction mixture was refluxed for 24 h. After evaporation of approximately half of the solvent, the mixture was poured into water (750 ml). The solid material was filtered and crystallized from ethanol to yield 7-(*N*-methylhexylamino)-thiophenoxy-2-nitrobenzoic acid **2.13** (24.8 g, 94% over two steps) as an orange solid. m.p. > 302°C, ^{1}H NMR δ 0.85-0.97 (m, 3H), 1.32 (m, 6H), 1.58-1.63 (m, 2H), 3.01 (s, 3H), 3.37 (t, *J* = 7.5 Hz, 2H), 6.75 (d, *J* = 8.7 Hz, 2H), 6.97 (d, *J* = 9.3 Hz, 1H), 7.35 (d, *J* = 8.7 Hz, 2H), 8.05 (dd, *J* = 9.0, 2.4 Hz, 1H), 8.95 (d, *J* = 2.7 Hz, 1H). ^{13}C NMR δ 14.35 (t), 22.99 (d), 26.89 (d), 27.06 (d), 31.93 (d), 38.66 (t), 52.90 (d), 113.38 (s), 125.63 (q): 127.36 (s), 133.04 (q), 134.06 (s), 137.50 (s), 144.04 (q), 150.74 (q), 156.94 (q), 166.05 (q).

7-(*N*-methylhexylamino)-2-nitro-9H-thioxanthene-9-one 2.14. To polyphosphoric acid (100 ml) at 50°C was added 7-(*N*-methylhexylamino)-thiophenoxy-2-nitrobenzoic acid **2.13** (8.2 g, 21.1 mmol). Under mechanical stirring, the mixture was heated at 130°C for 3 h and while hot poured into water (2 l). The solid material was filtered and washed with water until the washings were neutral followed by washing with hot toluene. After drying in vacuo 7-(*N*-methylhexylamino)-2-nitro-9H-thioxanthene-9-one **2.14** (4.36 g, 56%) was obtained as a brown solid. m.p. 135.7-136.1°C, ^{1}H NMR δ 0.85 (m, 3H), 1.32 (m, 6H), 1.59 (m, 2H), 3.01 (s, 3H), 3.37 (t, *J* = 7.2 Hz, 2H), 7.03 (dd, *J* = 8.7, 2.7 Hz, 1H), 7.32 (d, *J* = 9.3 Hz, 1H), 7.55 (d, *J* = 9.3 Hz, 1H), 7.62 (d, *J* = 3.0 Hz, 1H), 8.20 (dd, *J* = 8.7, 2.7 Hz,1H), 9.28 (d, *J* = 2.7 Hz,1H).^{13}C NMR δ 14.31 (t), 22.94 (d), 26.87 (d), 27.03 (d), 38.05 (t), 52.78 (d),

110.12 (s), 118.99 (s), 121.55 (q), 125.04 (s), 125.72 (s), 127.21 (s), 127.43 (s), 128.61 (q), 129.41 (q), 144.88 (q), 145.51 (q), 148.90 (q), 178.67 (q). HRMS calcd for $C_{20}H_{22}N_2O_3S_2$: 370.13509 found: 370.13422.

7-(*N*-methylhexylamino)-2-nitro-9H-thioxanthene-9-thione 2.6. 7-(*N*-methylhexylamino)-2-nitro-9H-thioxanthene-9-one **2.14** (4 g, 10.8 mmol) and Lawesson's reagent (5.84 g, 14.4 mmol) were dissolved in dry toluene (100 ml). The reaction mixture was refluxed for 2 h during which period the color of the mixture turned deep purple. The mixture was concentrated and pure thioketone **2.6** (3.05 g, 73%) was isolated as a purple solid after column chromatography with toluene (SiO_2, R_f = 0.68). m.p. 130.5-130.8°C, ^{1}H NMR δ 0.90 (m, 3H), 1.34 (m, 6H), 1.60 (m, 2H), 3.06 (s, 3H), 3.42 (t, *J* = 7.5 Hz, 2H), 7.18 (dd, *J* = 9.0, 3.0 Hz, 1H), 7.44 (d, *J* = 9.0 Hz, 1H), 7.66 (d, *J* = 9.0 Hz, 1H), 8.17 (d, J= 3.0 Hz, 1H), 8.27 (dd, *J* = 9.0, 2.7 Hz, 1H), 9.86 (d, *J* = 3.0 Hz, 1H). ^{13}C NMR δ 14.31 (t), 22.94 (d), 26.87 (d), 27.03 (d), 38.05 (t), 52.78 (d), 110.12 (s), 118.99 (s), 121.55 (q), 125.04 (s), 125.72 (s), 127.21 (s), 127.43 (s), 128.61 (q), 129.41 (q), 144.88 (q), 145.51 (q), 148.90 (q), 178.67 (q). HRMS calcd for $C_{20}H_{22}N_2O_2S_2$: 386.11225 found: 386.11156.

Dispiro[1,2,3,4-tetrahydrophenanthrene-4,2'-thiirane-3',9"-(7-*N*-hexylmethylamino)-2"-nitro))-9"H-thioxanthene 2.7. In a double Schlenck vessel, 2,3-dihydro-1H-naphtho[2,1-b]thiopyran-1-one hydrazone **2.5** (685 mg, 3 mmol) was dissolved in dry dichloromethane (75 ml) and $MgSO_4$ (1 g) was added. This mixture was cooled to -10°C and subsequently Ag_2O (1.1 g) and a saturated solution of saturated KOH in methanol (2.4 ml) were added. The mixture was allowed to warm to 0°C and it turned deep red at about -5°C. This deep red reaction mixture was filtered onto a deep green solution of 7-(*N*-methylhexylamino)-2-nitro-9H-thioxanthene-9-thione **2.6** (500 mg, 1.29 mmol) in dichloromethane (10 ml) upon which nitrogen evolution was visible and the green color rapidly disappeared. The mixture was stirred for an additional hour and then the solvent was evaporated. After column chromatography (SiO_2, CH_2Cl_2 : *n*-hexane 1:2, R_f = 0.38) to remove the byproducts 7-(*N*-methylhexylamino)-2-nitro-9H-thioxanthene-9-one (R_f = 0.26) and 2,3-dihydro-1*H*-benzo[*f*]thiochromen-1-one *N*-(2,3-dihydro-1*H*-benzo[*f*]thiochromen-1-ylidene)hydrazone, the azine product of two upper halves coupling together (R_f = 0.44), the episulfide **2.7** (640 mg, 85% relative to the amount of thioketone used) was obtained as a solid *cis* : *trans* mixture in the ratio of 60:40 (as determined by NMR). The two isomers were not separated but, to a large extent, could be identified separately by NMR. ^{1}H NMR δ 0.92 (m, 3H, *cis*-nitro), 1.10 (m, 3H, *trans*-nitro), 1.26-1.41 (m, 6H, *cis*- and *trans*-nitro), 1.60 (m, 2H, *cis*- and *trans*-nitro), 2.04 (s, 3H, *trans*-nitro), 2.18-2.24 (m, 2H, *trans*-nitro), 2.43-2.79 (m, 4H, *cis*- and *trans*-nitro), 3.02 (s, 3H, *cis*-nitro), 3.35-3.43 (m, 2H, *cis*-nitro), 6.18-6.24 (m, 2H, *trans*-nitro), 6.71 (dd, *J* = 2.4, 8.4 Hz, 1H, *cis*-nitro), 6.85 (d, *J* = 8.7 Hz, 1H, *trans*-nitro), 6.96 (d, *J* = 8.4 Hz, 1H, *cis*-nitro), 7.04 (m, 1H, *cis*- and *trans*-nitro), 7.23-7.64 (m, 7H *cis*-nitro, 6H *trans*-nitro), 7.85 (m, 1H, *cis*-nitro), 8.11 (dd, *J* = 8.4, 2.1 Hz, 1H, *trans*-nitro), 8.86 (d, *J* = 9 Hz, 1H, *trans*-nitro), 9.01 (m, 1H, *cis*-nitro). MS (EI): 584.8 [M+].

7-(N-methylhexylamino)-2-nitro-9-(1',2',3',4'-tetrahydrophenanthrene-4'ylide)-9H-thioxanthene 2.4. **Linear approach:** Dispiro[1,2,3,4-tetrahydrophenanthrene-4,2'-thiirane-3',9"-(7-*N*-hexylmethylamino)-2"-nitro))-9"H-thioxanthene **2.7** (550 mg, 0.94 mmol) was dissolved in *p*-xylene (50 ml) and Cu-bronze (3 g) was added. This mixture was refluxed for 24 h. The copper was removed by filtration over a short silica column which was washed with dichloromethane until the washings were colorless. After flash chromatography (SiO_2, *n*-hexane/CH_2Cl_2 2/1, R_f = 0.2)) a *cis*-*trans* mixture of 7-(*N*-methylhexylamino)-2-nitro-9-(1',2',3',4'-tetrahydrophenanthrene-4'ylide)-9H-thioxanthene **2.4** (410 mg, 79%) was obtained as an orange solid. The remaining was starting material which could be converted to the product by repeating the procedure. **Convergent approach:** A

solution of BINAP (6 mg, 0.096 mmol) and $Pd_2(dba)_3$ (3 mg, 0.0025 mmol) in dry toluene (50 ml) was stirred for half an hour at r.t. and the solution turned from dark red to dark orange. After this period NaO*t*Bu (50 mg, 1.3 mmol) was added, followed by bromosubstituted alkene **2.5** (41 mg, 0.079 mmol) and N-methylhexylamine (10 mg, 0.088 mmol). This solution was stirred overnight at 90°C . After this period the reaction mixture was poured onto CH_2Cl_2 (50 ml) and filtered. The solvents were evaporated. The crude product was dissolved in a small amount of CH_2Cl_2 and purified using column chromatography (SiO_2; CH_2Cl_2 : *n*-hexane : NEt_3 50 : 50 :1) to afford **2.4** as a orange solid (46 mg, 87%).

Resolution was performed on a Chiralcel OD HPLC column (5 μm; 250 × 4.6 mm) for preparative separation using *n*-heptane : 2-propanol (90 : 10) for *trans*-**2.4** (elution times: 5.46 min for (*M*)-*trans*-**2.4** and 7.88 min for (*P*)-*trans*-**2.4**). For *cis*-**2.4** *n*-heptane : 2-propanol (99 : 1) was used as eluent on the same chiral column to give (*M*)-*cis*-**2.4** after 10.46 min and (*P*)-*cis*-**2.4** (again not used for the experiments) after 12.67 min. For analytical HPLC the same column was used with *n*-heptane : 2-propanol (90 : 10) as an eluent: elution times were: (*M*)-*trans*-**2.4**: 7.88 min, (*M*)-*cis*-**2.4**: 5.68 min, (*P*)-*cis*-**2.4**: 6.10 min, (*P*)-*trans*-**2.4**: 7.88 min. m.p.$_{cis\text{-}\mathbf{2.4}}$ 133.4-133.9°C, m.p.$_{trans\text{-}\mathbf{2.4}}$ 140.0-140.4°C, ^{1}H NMR *trans*-isomer: δ 0.83-0.90 (m, 5H), 1.16-1.29 (m, 6H), 2.27 (s, 3H), 2.65-2.72 (m, 2H), 3.51-3.55 (m, 2H), 3.60-3.66 (m, 2H), 5.89 (d, *J* = 2.7 Hz, 1H), 6.22 (dd, *J* = 8.4, 2.7 Hz, 1H), 7.09-7.28 (m, 4H), 7.40 (d, *J* = 8.7 Hz, 1H), 7.47-7.64 (m, 2H), 7.71 (d, *J* = 8.7 Hz, 1H), 8.14 (dd, *J* = 2.7, 8.4 Hz, 1H), 8.41 (d, *J* = 2.4 Hz, 1H). *cis*-isomer: δ 0.83-0.93 (m, 5H), 1.26-1.35 (m, 6H), 3.02 (s, 3H), 3.28-3.45 (m, 2H), 3.51-3.66 (m, 2H), 3.82-3.89 (m, 2H), 6.70 (dd, *J* = 8.7, 2.7 Hz, 1H), 6.91 (d, *J* = 2.7 Hz, 1H), 6.99 (bt, *J* = 6.9 Hz, 1H), 7.07 (bt, *J* = 6.9 Hz, 1H), 7.28 (d, *J* = 2.7 Hz, 1H,), 7.39-7.47 (m, 4H), 7.55-7.62 (m, 3H). ^{13}C NMR *trans*-isomer: δ 14.29 (t), 22.85 (d), 23.95 (d), 24.78 (d), 29.52 (d), 29.86 (d), 30.20 (d), 31.73 (d), 32.09 (d), 37.98 (t), 52.75 (d), 111.91 (s), 111.78 (s), 117.33 (q), 121.58 (s), 122.39 (s), 124.30 (s), 124.76 (s), 125.16 (s), 126.03 (s), 126.10 (s), 126.88 (s), 127.78 (s), 128.11 (s), 131.58 (q), 132.99 (q), 134.00 (q), 134.37 (q), 135.10 (q), 135.36 (q), 136.66 (q), 137.43 (q), 145.86 (q), 146.25 (q), 148.29 (q). *cis*-isomer: δ 14.29 (t), 22.85 (d), 24.93 (d), 25.07 (d), 29.66 (d), 29.86 (d), 30.15 (d), 31.94 (d), 32.09 (d), 38.76 (t), 53.21 (d), 111.03 (s), 111.83 (s), 119.01 (q), 120.90 (s), 123.66 (s), 124.35 (s), 124.64 (s), 126.02 (s), 126.15 (s), 126.69 (s), 128.15 (s), 128.22 (s), 128.46 (s), 131.06 (q), 131.59 (q), 132.96 (q), 133.40 (q), 134.40 (q), 135.05 (q), 135.71 (q), 138.92 (q), 144.44 (q), 145.21 (q), 148.72 (q).

trans-**2.4**: UV (*n*-hexane): λ_{max} (ε) 258 (37703), 274 (31291), 320 (8246), 360 (6544), 410 (3548), (*P*)-*trans*-**2.4** CD (*n*-hexane): λ_{max} (Δε) 255 (-33.9), 275 (+33.5), 326 (+6.8), 352 (-3.7). *cis*-**2.4** UV (*n*-hexane): λ_{max} (ε) 256 (39030), 275 (28778), 298 (14849), 356 (5137), (*M*)-*cis*-**2.4** CD (*n*-hexane): λ_{max} (Δε) 256 (+22.8), 280 (-30.5), 323 (-2.7), 362 (5.2).

The crystal structure determination of *trans*-**2.4** was performed on a orange-red block of dimensions 0.06 × 0.20 × 0.25 mm obtained after crystallization from *n*-hexane and dichloromethane. Data: Triclinic, P-1, a = 9.189(5) Å, b = 10.354(6) Å, c = 15.877(6) Å; V = 1374.5(12) Å^3. Z = 2. T = 130 K. The structure was solved to a final R index of 0.041 for 8588 unique reflections.

The crystal structure determination of *cis*-**2.4** was performed on a irregular red block fragment of dimensions 0.31 × 0.23 × 0.11 mm obtained after crystallization from *n*-hexane and dichloromethane. Data: Triclinic, P-1, a = 10.0842(5) Å, b = 11.4814(6) Å, c = 12.2991(6) Å; V = 1378.42(12) Å^3. Z = 2. T = 110 K. The structure was solved to a final R index of 0.0339 for 7026 unique reflections.

HRMS calcd for $C_{33}H_{32}N_2O_2S_2$: 552.19050, found: 552.19255, anal. calcd: C 71.71, H 5.84, N 5.07, S 11.60, found: C 71.57, H 5.68, N 5.05, S 11.46.

2-[(4-Bromophenyl)sulfanyl]-5-nitrobenzoic acid 2.22 To a solution of $NaHCO_3$ (10.8 g, 128 mmol) in dry ethanol (200 ml) were added *p*-bromothiophenol (12 g, 64 mmol) and 2-chloro-5-nitrobenzoic acid (13.14 g, 64 mmol). The reaction mixture was refluxed for 24 h under a nitrogen atmosphere. After this period a 10% HCl solution (150 ml) was added, after which a precipitate was collected by filtration, yielding crude **2.22** (27.4 g) as a yellow solid which was subsequently used in the cyclization reaction to form **2.16**.

2-Bromo-7-nitro-9H-thioxanthen-9-one 2.16. A suspension of **2.22** (27.4 g, crude) in sulfuric acid (400 ml) was stirred and heated at 100°C for 3 h. The suspension was then poured onto ice (500 g) and left overnight. Next the precipitate was filtered and washed with water (2 x 50 ml), concentrated $NaHCO_3$ (2 x 100 ml) and ethanol (2 x 50 ml). The yellow solid was dried at 60°C under reduced pressure, yielding **2.16** (20.2 g, 95%). m.p. 288.1-290.5°C, ^{1}H NMR : δ 7.46 (d, *J* = 8.4 Hz, 1H), 7.70 (d, *J* = 8.8 Hz, 1H), 7.76 (dd , *J* = 8.4, 2.2 Hz , 1H), 8.39 (dd, *J* = 9.2, 2.6 Hz , 1H), 8.72 (d, *J* = 2.2 Hz, 1H), 9.38 (d, *J* = 2.19 Hz, 1H). No ^{13}C data available due to low solubility. HRMS calcd for $C_{13}H_6BrNO_3S$: 334.92512, found: 334.92661.

2-Bromo-7-nitro-9H-thioxanthene-9-thione 2.23, A suspension of xanthone **2.16** (5.1 g, 15 mmol) and P_2S_5 (8 g, 36 mmol) in dry toluene (150 ml) was refluxed for 72 h. After this period additional P_2S_5 (3 g, 14 mmol) was added and the suspension was refluxed for another 3 h. The solution was then allowed to cool to about 50°C and filtered. The flask was washed with hot toluene until the solvent was no longer green. From the filtered solution the solvent was evaporated to leave a brown solid. This solid was recrystallized from toluene to give dark brown crystals, yielding **2.23** (4.0 g, 76%). m.p. 274.8-276.3°C, ^{1}H NMR : δ 7.43 (d, *J* = 8.4 Hz, 1H), 7.66 (d, *J* = 8.8 Hz, 1H), 7.73 (dd, *J* = 8.4, 2.2 Hz , 1H), 8.34 (dd, *J* = 9.2, 2.6 Hz, 1H), 9.00 (d, *J* = 2.2 Hz, 1H), 9.68 (d, *J* = 2.6 Hz, 1H). No ^{13}C data available due to low solubility. HRMS calcd for $C_{13}H_6BrNO_2S_2$: 350.90228, found: 350.90238.

Dispiro[1,2,3,4-tetrahydrophenanthrene-4,2'-thiirane-3',9"-7-bromo-2"-nitro))-9"H-thioxanthene 2.24. A stirred solution of hydrazone **2.5** (350 mg, 1.53 mmol) in dry CH_2Cl_2 (20 ml) was cooled to -20°C, whereupon $MgSO_4$ (600 mg), Ag_2O (531 g, 2.29 mmol) and a saturated solution of KOH in dry MeOH (1.2 ml) were successively added and the mixture was stirred at this temperature under a nitrogen atmosphere. After the solution turned deep red it was filtered into another ice-cooled bulb containing thioketone **2.23** (445 mg, 1.53 mmol) and the mixture was then stirred for another 3 h while warming up to room temperature. The precipitated solid (excess **2.23**) was filtered off and the solvent was evaporated. The product was purified by column chromatography (SiO_2, CH_2Cl_2 : hexane 1:1), yielding **2.24** (510 mg, 60.1%) as a yellow powder and a mixture of *cis*- and *trans*-isomers. HRMS calcd for $C_{26}H_{16}BrNO_2S_3$: 550.95060 found: 550.95225.

7-Bromo-2-nitro-9-(1',2',3',4'-tetrahydrophenanthrene-4'ylidene)-9H-thioxanthene 2.15. Episulfide **2.24** (0.510 g, 0.92 mmol) was dissolved in toluene (50 ml). Triphenylphosphine (0.39 g, 1.5 mmol) was added and the resulting solution was refluxed for 3 d. The solvent was evaporated and the resulting orange solid was recrystallized from 96% EtOH to yield **2.15** as a mixture of isomers as a yellow powder (491 mg, 97%). ^{1}H NMR : δ 2.30-2.40 (m, 3H), 3.45-3.64 (m, 8H), 6.53 (d, *J* = 1.8 Hz, 1H), 6.87-7.16 (m, 10H), 7.32-7.71 (m, 22H), 8.14 (dd, *J* = 8.4, 2.2 Hz, 1H), 8.37 (d, *J* = 2.2 Hz,

1H). MS (EI): 519 [M+]. HRMS calcd for $C_{26}H_{16}BrNO_2S_2$: 518.97853, found 518.97674, anal. calcd: C 60.24, H 3.11, N 2.70, S 12.37, found: C 60.33, H 3.05, N 2.86, S 12.69.

7-(N-methylphenyl-amino)-2-nitro-9-(1',2',3',4'-tetrahydrophenanthrene-4'ylidene)-9H-thioxanthene 2.19. A solution of BINAP (6 mg, 0.096 mmol) and $Pd_2(dba)_3$ (3 mg, 0.0025 mmol) in dry toluene (50 ml) was stirred for half an hour at RT and the solution turned from dark red to dark orange. After this period NaO*t*Bu (50 mg, 1.3 mmol) was added, followed by bromo-substituted alkene **2.4** (41 mg, 0.079 mmol) and N-methylaniline (10 mg, 0.088 mmol). This solution was stirred overnight at 90°C . After this period the reaction mixture was poured into CH_2Cl_2 (50 ml) and filtered. The solvents were evaporated. The crude product was dissolved in a small amount of CH_2Cl_2 and purified using column chromatography (SiO_2, CH_2Cl_2 : *n*-hexane : NEt_3 50 : 50 :1) to afford **2.19** (38 mg, 87% yield) as a orange solid consisting of *cis*- and *trans*-isomers. ^{1}H NMR : δ 2.15-2.35 (m, 2H), 2.49 (s, 3H), 2.78-2.97 (m, 2H), 3.23 (t, *J* = 9.2 Hz, 2H), 3.32 (s, 3H), 3.40-3.64 (m, 2H), 6.16 (d, *J* = 2.2 Hz, 1H), 6.27 (d, *J* = 8.4 Hz, 2H), 6.39 (dd, *J* = 5.9, 2.6 Hz, 1H), 6.78-7.20 (m, H), 7.28-7.72 (m, H), 8.11 (dd, *J* = 8.4, 2.2 Hz, 1H), 8.35 (d, *J* = 2.2 Hz, 1H). MS (EI): 544 [M+]

HPLC analysis yielded the relative ratios of the different enantiomers. Using a Chiralcel OD column with *n*-heptane : 2-propanol 95 : 5 as an eluent the elution times were 10.32 min for the first *trans*-isomer (the configuration was not assigned), 11.42 min for the second *trans*-isomer, 15.29 min for the first *cis*-isomer and 16.89 min for the second *cis*-enantiomer.

7-Xylyl-2-nitro-9-(1',2',3',4'-tetrahydrophenanthrene-4'ylide)-9H-thioxanthene 2.20. Racemic 7-bromo-2-nitro-9-(1',2',3',4'-tetrahydrophenanthrene-4'ylidene) -9H-thioxanthene **2.5** (40.0 mg, 77 μmol) and palladium tetrakistriphenylphosphine (11.3 mg, 10 μmol) were dissolved in DME (5 ml) and stirred for 10 min to allow Pd complex formation. Subsequently, xylyl boronic acid (13 mg, 85 μmol) and $Ba(OH)_2 \cdot 8H_2O$ (40 mg, 127 μmol) in water (5 ml) were added. The mixture was stirred and refluxed for 18 h and cooled to room temperature. The product was extracted twice with ether (10 ml) and dichloromethane (10 ml) and the combined fractions were dried over magnesium sulphate. Evaporation of the solvents yielded crude 7-xylyl-2-nitro-9-(1',2',3',4'-tetrahydrophenanthrene-4'ylide)-9H-thioxanthene **2.20** (28 mg, 67%) as a bright yellow solid. One *trans*-isomer was readily separated by chiral HPLC (Chiralcel OD, *n*-hexane : isopropanol 99 : 1, retention times: first *trans* fraction: 15.4 min , overlapping *cis* fractions: 17.7 and 18.8 min, second *trans* fraction: 22.1 min). m.p.$_{trans\text{-}\mathbf{2.20}}$ 278.0-279.8°C, *trans*-nitro-**2.20**: ^{1}H NMR δ 0.70 (s, 3H), 1.71 (s, 3H), 2.16-2.27 (m, 1H), 3.47-3.61 (m, 3H), 6.48-6.49 (d, *J* = 1.5 Hz, 1H), 6.64-6.67 (dd, *J* = 8.1, 1.8 Hz, 1H), 6.80-6.82 (d, *J* = 7.3 Hz, 1H), 6.89-6.91 (d, *J* = 7.3 Hz, 1H), 6.98-7.03 (t, *J* = 7.5 Hz, 1H), 7.11-7.21 (m, 2H), 7.32-7.35 (d, *J* = 8.8 Hz, 1H), 7.42-7.44 (d, *J* = 8.1 Hz, 1H), 7.58-7.61 (d, *J* = 8.4 Hz, 1H), 7.59-7.62 (d, *J* = 7.0 Hz, 1H), 7.68-7.70 (d, *J* = 8.4 Hz, 1H), 7.77-7.80 (d, *J* = 8.4 Hz, 1H), 8.18-8.22 (dd, *J* = 8.8, 2.2 Hz, 1H), 8.43-8.44 (d, *J* = 2.2 Hz, 1H). No spectral information on pure *cis*-nitro-**2.20** from the ^{1}H-NMR spectrum of a *cis*-*trans* mixture . The following signals can be assigned to the *cis*-**2.20** δ 1.98 (s, 3H), 2.22 (s, 3H), 2.27-2.43 (m, 1H), 3.38-3.65 (m, 3H), 6.95-7.75 (m, 1H). *Cis*-*trans* mixture **2.20**: ^{13}C-NMR δ 19.7 (q), 20.6 (q), 20.9 (q), 21.1 (q), 29.4 (t), 29.5 (t), 29.7 (t), 30.0 (t), 121.0 (d), 121.7 (d), 122.4 (d), 123.3 (d), 124.0 (d), 124.3 (d), 124.5 (d), 124.7 (d), 125.97 (d), 126.01 (d), 126.6 (d), 126.7 (d), 126.8 (d), 126.9 (d), 127.5 (d), 127.6 (d), 127.6 (d), 127.8 (d), 128.1 (d), 128.3 (d), 128.4 (d), 128.5 (d), 129.3 (d), 130.7 (s), 131.4 (s), 131.6 (s), 131.9 (s), 132.0 (s), 132.2 (s), 132.97 (s), 132.98 (s), 134.6 (s), 134.7 (s), 134.9 (s), 135.3 (s), 135.4 (s), 135.7 (s), 135.7 (s), 136.0 (s), 136.2 (s), 136.7 (s), 137.2 (s), 138.5 (s), 140.10 (s), 140.13 (s), 140.2 (s), 140.4 (s), 142.7 (s), 144.8 (s), 145.4 (s), 146.2 (s). Due to overlap in the region from 120 to 130 ppm, 7 signals out of 30 for tertiary carbons are missing. Due to overlap in the region from 130 to 145, 2 signals out of 30 for quartenary

are missing. HRMS calcd for $C_{34}H_{25}NO_2S_2$: 543.13265, found: 543.13191, anal. calcd: C 75.11, H 4.45, N 2.58, found: C 74.81, H 4.33, N 2.62.

2-Nitro-9H-thioxanthene-9-thione 2.25. This compound was synthesized by Ben de Lange.[18] The corresponding ketone can be synthesized in two steps from thiophenol.[26] Thioketone **2.25** was readily obtained by a P_2S_5 thioketone formation. ^{1}H NMR δ 7.48 (ddd, *J* = 8.4, 8.1, 1.1 Hz, 1H), 7.57 (dd, *J* = 8.1, 1.1 Hz, 1H), 7.64-7.69 (m, 1H), 7.70 (d, *J* = 8.8 Hz, 1H), 8.35 (dd, *J* = 8.8, 2.2 Hz, 1H), 8.90 (dd, *J* = 8.4, 1.1 Hz, 1H), 9.75 (d, *J* = 2.2 Hz, 1H). HRMS calcd. for $C_{13}H_7NO_2S_2$: 272.992, found: 272.991.

Dispiro[1,2,3,4-tetrahydrophenanthrene-4,2'-thiirane-3',9"-2-nitro-9"H-thioxanthene In a double Schlenck vessel 2,3-dihydro-1H-naphtho[2,1-b]thiopyran-1-one hydrazone **2.5** (1.75 g, 7.65 mmol) was dissolved in dry dichloromethane (75 ml) and $MgSO_4$ (2.5 g) was added. This mixture was cooled to -10°C and subsequently Ag_2O (2.65 g) and saturated KOH in methanol (6 ml) were added. The mixture was allowed to warm to 0°C and it turned deep red at about -5°C. This deep red reaction mixture was filtered onto a deep green solution of 2-nitro-9H-thioxanthene-9-thione **2.25** (860 mg, 3.15 mmol) in dichloromethane (10 ml) upon which nitrogen evolution was visible and the green color rapidly disappeared. The mixture was stirred for an additional hour and then the solvent was evaporated. Washing the solid product with ethanol yielded the desired episulfide (625 mg, 42%) as a yellow solid; no further optimization nor resolution was performed.

2-Nitro-9-(1',2',3',4'-tetrahydrophenanthrene-4'ylide)-9H-thioxanthene 2.26. Dispiro[1,2,3,4-tetrahydrophenanthrene-4,2'-thiirane-3',9"-2-nitro))-9"H-thioxanthene (625 mg, 1.33 mmol) was dissolved in *p*-xylene (50 ml) and Cu-bronze (3 g) was added. This mixture was refluxed for 24 h. The copper was filtered off over a short silica column which was washed with dichloromethane until the washings were colorless. Evaporation of the solvent yielded a *cis*-*trans* mixture of 7-nitro-9-(1',2',3',4'-tetrahydrophenanthrene-4'ylide)-9H-thioxanthene **2.4** (410 mg, 79%). The *cis*- and *trans*-isomers were resolved by flash chromatography (SiO_2, CH_2Cl_2 / *n*-hexane 1/2, R_f = 0.20 (*trans*), 0.13 (*cis*)). *trans*-nitro: ^{1}H NMR δ 3.50-3.66 (m, 4H), 6.52 (bd, *J* = 4.2 Hz, 2H), 6.81-6.88 (m, 1H), 7.02 (bt, *J* = 7.8 Hz, 1H), 7.14 (bt, *J* = 7.8 Hz, 1H), 7.33 (d, *J* = 7.5 Hz, 1H), 7.42 (d, *J* = 8.7 Hz, 1H), 7.49 (d, *J* = 8.4 Hz, 1H), 7.59 (d, *J* = 8.1 Hz, 1H), 7.58 (d, *J* = 8.7 Hz, 1H), 7.75 (d, *J* = 8.7 Hz, 1H), 8.18 (dd, *J* = 8.4, 2.1 Hz, 1H), 8.43 (d, *J* = 2.1 Hz, 1H). *cis*-nitro: ^{1}H NMR δ 3.00-3.12 (m, 2H), 3.42-8.78 (m, 2H), 6.32 (d, *J* = 7.5 Hz, 1H), 6.87 (t, *J* = 7.5 Hz, 1H), 7.17 (d, *J* = 2.1 Hz, 1H), 7.20 (d, *J* = 7.5 Hz, 1H), 7.51-7.62 (m, 8H), 8.02 (dd, *J* = 8.7 Hz, 1H). Due to extremely low solubility no ^{13}C-NMR analysis was performed. HRMS calcd for $C_{26}H_{17}NO_2S_2$: 439.07005 found: 439.06810, anal. calcd: C 71.05, H 3.90, N 3.19, S 14.59, found: C 70.72, H 3.79, N 3.22, S 14.49. HPLC analysis yielded the relative ratio of the different enantiomers, using a Chiralcel OD column with *n*-heptane : 2-propanol (99 : 1) as an eluent. The elution times were 13.24 min for the first *trans*-isomer (the configuration is not assigned), 16.44 min for the second *trans*-isomer, 18.43 min for the first *cis*-isomer and 22.91 min for the second *cis*-isomer.

2-(N,N-dimethylamino)-9H-thioxanthene-9-thione (2.27). Thioketone **2.27** was prepared from the corresponding ketone which was synthesized by J. de Jong.[27] This synthesis is comparable to the synthesis of compound **2.14** when N,N-dimethylaniline and 2-iodobenzoic acid are used instead of N,N-methylhexylaniline and 2-chloro-5-nitrobenzoic acid. Ketone 2-(N,N-dimethylamino)-9H-thioxanthene-9-one (2.1 g, 8.4 mmol) was dissolved in dry toluene (100 ml) and Lawessons reagent (5.1 g, 12.5 mmol) was added. This solution was refluxed for 3 h. The mixture was concentration and pure thioketone **2.27** (1.2 g, 47%) was isolated pure as a purple solid after column chromatography

with toluene (SiO_2). ^{1}H-NMR δ 3.04 (s, 3H), 7.10 (dd, *J* = 8.7, 2.2 Hz, 1H), 7.42 (m, 2H), 7.55 (m, 2H), 7.86 (d, 2.2 Hz, 1H), 8.64 (d, *J* = 8.7 Hz, 1H).

Dispiro[1,2,3,4-tetrahydrophenanthrene-4,2'-thiirane-3',9"-(2-N,N-dimethylamino)-9"H-thioxanthene. In a double Schlenck vessel, 2,3-dihydro-1H-naphtho[2,1-b]thiopyran-1-one hydrazone **2.5** (171 mg, 260 μmol) was dissolved in dry dichloromethane (10 ml) and $MgSO_4$ (250 mg) was added. This mixture was cooled to -10°C and subsequently Ag_2O (242 mg) and saturated KOH in methanol (0.5 ml) were added. The mixture was allowed to warm to 0°C and it turned deep red at about -5°C. This deep red reaction mixture was filtered onto a deep green solution 2-(N,N-dimethylamino)-9H-thioxanthene-9-thione **2.27** (70 mg, 260 μmol) in dichloromethane (10 ml) upon which nitrogen evolution was visible and the green color rapidly disappeared. The mixture was stirred for an additional hour and then the solvent was evaporated. After purification by column chromatography (SiO_2, dichloromethane / *n*-hexane 1 : 1, R_f = 0.5) the product was obtained as a solid (152 mg, 43%). No resolution was performed of the *cis*- and *trans*-isomers of dispiro[1,2,3,4-tetrahydrophenanthrene-4,2'-thiirane-3',9"-(2-N,N-dimethylamino)-9"H-thioxanthene.

2--(N,N-dimethylamino)-9-(1',2',3',4'-tetrahydrophenanthrene-4'ylide)-9H-thioxanthene 2.28. The total amount of dispiro[1,2,3,4-tetrahydrophenanthrene-4,2'-thiirane-3',9"-(2-N,N-dimethylamino)-9"H-thioxanthene (152 mg, 320 μmol) was dissolved of *p*-xylene (25 ml). To this solution triphenylphosphine (126 mg, 0.48 mmol) was added and this mixture was refluxed overnight. Evaporation of the solvent yielded a brown solid mixture of triphenylphosphine and 2-(N,N-dimethylamino)-9-(1',2',3',4'-tetrahydrophenanthrene-4'ylide)-9H-thioxanthene **2.28** as a brown solid. After flash chromatography (SiO_2, CH_2Cl_2 / *n*-hexane 1/2, R_f = 0.18 (*trans*), R_f = 0.10 (*cis*)) the *trans*-isomer was obtained pure. The *cis* and *trans* fractions combined to 133 mg (95%) of **2.28**. *Trans*-**2.28**: ^{1}H NMR δ 3.02 (s, 6H), 3.52-3.65 (m, 2H), 3.83-3.88 (m, 2H), 6.43 (dt, *J* = 7.5 Hz, 1H), 6.54 (bd, *J* = 7.5 Hz, 1H), 6.71-6.76 (m, 2H), 6.98 (d, *J* = 2.4 Hz, 1H), 7.03 (d, *J* = 8.4 Hz, 1H), 7.13 (t, *J* = 7.5 Hz, 1H), 7.32-7.48 (m, 2H), 7.57 (d, *J* = 8.4 Hz, 1H), 7.61 (d, *J* = 9.0 Hz, 1H), 7.71 (d, *J* = 6.9 Hz, 1H), 7.75 (d, *J* = 6.9 Hz, 1H). Due to tailing on the column no pure *cis* material is obtained; some additional NMR signals for the mixture of *cis* and *trans* are highly indicative for the *cis*-configuration: ^{1}H NMR δ 2.25 (s, 3H), 5.96 (d, *J* = 2.7 Hz, 1H), 6.24 (dd, *J* = 8.8, 2.7 Hz, 1H), the rest of the absorptions strongly overlap with those of the *trans*-compound. HRMS calcd for $C_{28}H_{23}NO_2S_2$: 437.12719 found: 437.11021 HPLC analysis yielded the relative ratio of the different enantiomers, using a Chiralcel OD column with *n*-heptane : 2-propanol 99 : 1 as an eluent the elution times were 7.64 min for the first *trans*-isomer (the configuration was not assigned), and 9.15 min for the first *cis*-isomer, 9.86 min for both the overlapping second *trans*- and *cis*-isomers.

2.7 References and Notes

1. S.L. Gilat, S. H. Kawai, J.-M. Lehn, *Chem. Eur. J.* **1995**, *1*, 275
2. W.F. Jager, J.C. de Jong, B. de Lange, N.P.M. Huck, A. Meetsma, B.L. Feringa, *Angew. Chem., Int. Ed. Engl.* **1995**, *34*, 348.
3. A.M. Schoevaars, *Ph.D. Thesis*, University of Groningen, **1998**.
4. H. Maskill, *The Physical Basis of Organic Chemistry*, Oxford Science Publications, New York, **1985**.
5. E.W. Meijer, B.L. Feringa, *Mol. Cryst. Liq. Cryst.* **1993**, *234*, 451.

[6] a) Z.F. Liu, A. Hashimoto, A. Fujishima, *Nature* **1990**, *347*, 658, b) T. Iyoda, T. Saika, K. Honda, T. Shimidzu, *Tetrahedron Lett.* **1989**, *30*, 5429, c) L. Gobbi, P. Seiler, F. Diederich, *Angew. Chem., Int. Ed. Engl.* **1999**, *38*, 674, d) H. Spreitzer, J. Daub, *Chem. Eur. J.* **1996**, *2*, 1150.

[7] a) S.H. Kawai, S.L. Gilat, J.-M. Lehn, *J. Chem. Soc. Chem. Commun.*, **1994**, 1011, b) H. Spreitzer, J. Daub, *Liebigs Ann.* **1995**, 1637, c) H. Görner, C. Fischer, J. Daub, *J. Photochem. Photobiol., A. Chem.* **1995**, *85*, 217, d) M. Irie, O. Miyatake, K. Uchida, *J. Am. Chem. Soc.* **1992**, *114*, 8715.

[8] N.P.M. Huck, B.L. Feringa, *J. Chem. Soc., Chem. Commun.* **1995**, 1095.

[9] Depending on the photostationary state a higher or lower emission is observed.

[10] R.A. van Delden, N.P.M. Huck, J.M. Warman, S.C.J. Meskers, H.P.J.M. Dekkers, B.L. Feringa, *J. Am. Chem. Soc.*, submitted for publication.

[11] T. Inada, S. Uchida, Y. Yokoyama, *Chem. Lett.* **1997**, 321.

[12] H. Okamoto, H.P.J.M. Dekkers, K. Satake, M. Kimura, *Chem. Commun.* **1998**, 1049.

[13] a) G.M. Tsivgoulis, J.-M. Lehn, *Chem. Eur. J.* **1996**, *2*, 1399, b) G.M. Tsivgoulis, J.-M. Lehn, *Angew. Chem., Int. Ed Engl.* **1995**, *34*, 1119.

[14] R.A. van Delden, A.M. Schoevaars, B.L. Feringa, *Mol. Cryst. Liq. Cryst*. **2000**, *344*, 1.

[15] W. Schuddeboom, S.A. Jonker, J.M. Warman, M.P. de Haas, M.J.W. Vermeulen, W.F. Jager, B. de Lange, B.L. Feringa, R.W. Fessenden, *J. Am. Chem. Soc.* **1993**, *115*, 3286.

[16] B.L. Feringa, W.F. Jager, B. de Lange, E.W. Meijer, *J. Am. Chem. Soc.* **1991**, *113*, 5468.

[17] reference 2: chapter 4.

[18] B. de Lange, *Ph.D. Thesis*, University of Groningen, **1993**.

[19] a) D.H.R. Barton, B.J. Willis, *J. Chem. Soc., Chem. Commun.* **1970**, 1225, b) R.M. Kellogg, J. Buter, S. Wassenaar, *J. Org. Chem.* **1972**, *37*, 4045.

[20] a) B. de Lange, W.F. Jager, B.L. Feringa, *Mol. Cryst. Liq. Cryst.* **1992**, *216*, 397; b) W.F. Jager, B. de Lange, B.L. Feringa, *Mol. Cryst. Liq. Cryst.* **1992**, *216*, 401.

[21] See for example: J.P Wolfe, S.L. Buchwald, *J. Org. Chem.* **2000**, *65*, 1144.

[22] A.M. Schoevaars, *personal communication*.

[23] J.F. Hartwig, F. Paul *J. Am. Chem. Soc.* **1995**, *117*, 5373.

[24] a) M.S. Driver, J.F. Hartwig *J. Am. Chem. Soc.* **1995**, *117*, 4708. b) M.S. Driver, J.F. Hartwig *J. Am. Chem. Soc.* **1997**, *119*, 8232.

[25] N.P.M. Huck, *PhD. Thesis*, University of Groningen, **1997**.

[26] E.D. Amstutz, C.R. Neumoyer, *J. Am. Chem. Soc.* **1947**, *69*, 1922.

[27] J.C. de Jong, *internal communication*.